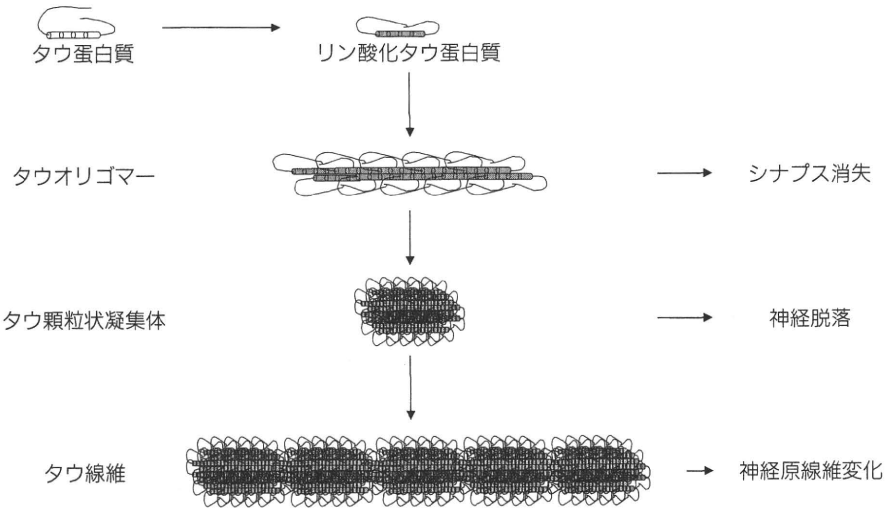

Fig. 5　タウの凝集体形成機構と神経変性の関係

ら精製された顆粒状凝集体は，予想どおり過剰にリン酸化されたタウ蛋白質で構成されていた。すなわち，試験管内の観察同様，ヒト脳の神経細胞において微小管から離れたタウ蛋白質は過剰にリン酸化され，顆粒状凝集体から神経原線維変化へと変化していくのである。

Ⅸ．タウ蛋白凝集体と神経変性

われわれは野生型タウ発現による脳機能変化を調べるため，前脳領域特異的な alpha CaMKII プロモーター下で野生型 4R2N ヒトタウ蛋白を過剰発現する Tg マウスを作製し，行動実験・MRI・免疫組織化学の手法により，Tg マウスの加齢に伴う脳機能の変化とタウの関係を調べた[23]。この Tg マウスは老齢期においても神経原線維変化も，神経脱落も示さない。12 カ月齢では学習障害を示さないが，老齢期（25 カ月齢）において Morris water maze による場所（空間）学習課題における学習記憶障害が観察された。このマウスの機能障害部位を検索する目的で，Mn-enhanced MRI 法を用いて空間学習時のマウスの脳活動パターンを測定した。その結果，学習能力の低下と嗅内野における神経活動が有意に相関し，老化した嗅内野の神経活動の低下が観察された。さらに，その部位では老化したマウスではシナプス消失が起こっていた。このマウスでは微小管に結合しているタウ蛋白量に 12，25 カ月齢の間で変化はなく，タウ過剰発現に伴う軸索輸送障害の関与の可能性は少ないと考えられる。リン酸化タウの免疫組織化学では，不活性化部位のニューロン（嗅内野）で老化に伴って特異的に PHF1 サイト（Ser396，404）がリン酸化されたタウ蛋白の蓄積が見出された。これらのことから，野生型タウ Tg マウスにおける加齢に伴う学習障害は神経原線維変化形成や神経脱落ではなく，タウの PHF1 サイトを含む過剰リン酸化が関与することが明らかになった。これはつまり，可溶性の過剰リン酸化タウはシナプス消失に関与することを示唆している。

一方，FTDP-17 のタウ変異である P301L は，タウ凝集がしやすい変異である。この変異を持つヒトタウ蛋白を，野生型タウ Tg マウスと同様のプロモーターを用いてマウス脳に発現する Tg マウスを作製し調べた。このマウスでは，不溶性タウの蓄積が観察される。しかしながら，ガリアス銀染色で特異的にみられる神経原線維変化の出現は非常に稀であった。実際に神経細胞数をカウントすると，P301L マウスで神経細胞の脱落が観察された。このことは，不溶性タウ凝集体の形成は神経脱落に関与することを示唆している。ヒト患者と同様，P301L タウのリン酸化程度は野生型タウと比べて低く，P301L タウの凝集体形成はリン酸化程度に依存しないと考えられる。不溶性タウ凝集体には顆粒状タウ凝集体，線維が含まれる。Santacruz ら[19]の結果からは，神経原線維変化と神経脱落は直接関係せず，神経原線維変化形成過程に神経毒性を示す凝集物があることが示唆されている。このことから，タウ線維になる前の凝集物である顆粒状タウ凝集体が神経細胞脱落の要因であることが示唆された（Fig. 5）。

おわりに

AD の病理学的特徴である Aβ 蓄積と神経原線維変化

についてこれまで多くの研究がなされ，Aβ仮説に従って治療法の検討が行われている。タウ研究から明らかになってきたことで，タウが過剰にリン酸化され微小管から乖離し，互いに重合を始めることがわかった。この過剰リン酸化タウによりシナプス消失が起こり，神経機能低下を引き起こす。さらに，顆粒状タウ凝集体を形成し始めると神経脱落が生じ，神経機能が不可逆的に低下することになる。顆粒状凝集物が線維化すると，無害な神経原線維変化として神経細胞内に残る。シナプス消失，神経脱落はADの機能低下を現す重要な要因であり，この2つにタウの変化が寄与していることになる。すなわち，タウはADにおける認知症を引き起こす執行役として作用していると考えられる。現在，タウ凝集阻害剤の1つであるメチレンブルーがAD患者の認知機能低下を阻害するという結果が報告されており[35]，この考えを支持している。

文　献

1) Shiarli AM, Jennings R, ShiJ, Bailey K, Davidson Y,et al: Comparison of extent of tau pathology in patients with frontotemporal dementia with Parkinsonism linked to chromosome 17 (FTDP-17), frontotemporal lobar degeneration with Pick bodies and early onset Alzheimer's disease. Neuropathol Appl Neurobiol **32**: 374-387, 2006
2) Braak H, Braak E: Evolution of the neuropathology of Alzheimer's disease. Acta Neurol Scand Suppl **165**: 3-12, 1996
3) Braak H, Braak E: Diagnostic criteria for neuropathologic assessment of Alzheimer's disease. Neurobiol Aging **18**: S85-S88, 1997
4) Holmes C, Boche D, Wilkinson D, Yadegarfar G, Hopkins V, et al: Long-term effects of Abeta42 immunisation in Alzheimer's disease: follow-up of a randomised, placebo-controlled phase I trial. Lancet **372**: 216-223, 2008
5) Goedert M, Jakes R: Expression of separate isoforms of human tau protein: correlation with the tau pattern in brain and effects on tubulin polymerization. EMBO J **9**: 4225-4230, 1990
6) Goedert M, Spillantini MG, Jakes R, Rutherford D, Crowther RA: Multiple isoforms of human microtubule-associated protein tau: sequences and localization in neurofibrillary tangles of Alzheimer's disease. Neuron **3**: 519-526, 1989
7) Lee G: Tau and src family tyrosine kinases. Biochim Biophys Acta **1739**: 323-330, 2005
8) Lee G, Thangavel R, Sharma VM, Litersky JM, Bhaskar, K, et al: Phosphorylation of tau by fyn: implications for Alzheimer's disease. J Neurosci **24**: 2304-2312, 2004
9) Lee G, Newman ST, Gard DL, Band H. Panchamoorthy G: Tau interacts with src-family non-receptor tyrosine kinases. J Cell Sci **111**: 3167-3177, 1998
10) Goedert M, Spillantini MG: Tau mutations in frontotemporal dementia FTDP-17 and their relevance for Alzheimer's disease. Biochim Biophys Acta **1502**: 110-121, 2000
11) Hutton M: Molecular genetics of chromosome 17 tauopathies. Ann N Y Acad Sci **920**: 63-73, 2000
12) Hutton M: Missense and splice site mutations in tau associated with FTDP-17: multiple pathogenic mechanisms. Neurology **56**: S21-S25, 2001
13) Spillantini MG, Crowther RA, Kamphorst W, Heutink P, van Swieten JC: Tau pathology in two Dutch families with mutations in the microtubule-binding region of tau. Am J Pathol **153**: 1359-1363, 1998
14) Spillantini MG, Goedert M: Tau protein pathology in neurodegenerative diseases. Trends Neurosci **21**: 428-433, 1998
15) van Swieten JC, Rosso SM, van Herpen E, Kamphorst W, Ravid R, et al: Phenotypic variation in frontotemporal dementia and parkinsonism linked to chromosome 17. Dement Geriatr Cogn Disord **17**: 261-264, 2004
16) Ingram EM, Spillantini MG: Tau gene mutations: dissecting the pathogenesis of FTDP-17. Trends Mol Med 8: 555-562, 2002
17) Gomez-Isla T, Hollister R, West H, Mui S, Growdon JM, et al: Neuronal loss correlates with but exceeds neurofibrillary tangles in Alzheimer's disease. Ann Neurol **41**: 17-24, 1997
18) Rapoport M, Dawson HN, Binder LI, Vitek MP, Ferreira A: Tau is essential to beta -amyloid-induced neurotoxicity. Proc Natl Acad Sci U S A **99**: 6364-6369, 2002
19) Santacruz K, Lewis J, Spires T, Paulson J, Kotilinek L, et al: Tau suppression in a neurodegenerative mouse model improves memory function. Science **309**: 476-481, 2005
20) Ebneth A, Godemann R, Stamer K, Illenberger S, Trinczek B, et al: Overexpression of tau protein inhibits kinesin-dependent trafficking of vesicles, mitochondria, and endoplasmic reticulum: implications for Alzheimer's disease. J Cell Biol **143**: 777-794, 1998
21) Santarella RA, Skiniotis G, Goldie KN, Tittmann P, Gross H,et al: Surface-decoration of microtubules by human tau. J Mol Biol **339**: 539-553, 2004
22) Seitz A, Kojima H, Oiwa K, Mandelkow EM, Song YH, et al: Single-molecule investigation of the inter-

ference between kinesin, tau and MAP2c. EMBO J **21**: 4896-4905, 2002
23) Kimura T, Yamashita S, Fukuda T, Park JM, Murayama M, et al: Hyperphosphorylated tau in parahippocampal cortex impairs place learning in aged mice expressing wild-type human tau. EMBO J **26**: 5143-5152, 2007
24) Shahani N, Subramaniam S, Wolf T, Tackenberg C, Brandt R: Tau aggregation and progressive neuronal degeneration in the absence of changes in spine density and morphology after targeted expression of Alzheimer's disease-relevant tau constructs in organotypic hippocampal slices. J Neurosci **26**: 6103-6114, 2006
25) Alonso AC, Grundke-Iqbal I, Iqbal K: Alzheimer's disease hyperphosphorylated tau sequesters normal tau into tangles of filaments and disassembles microtubules. Nat Med **2**: 783-787, 1996
26) Alonso AC, Zaidi T, Grundke-Iqbal I, Iqbal K: Role of abnormally phosphorylated tau in the breakdown of microtubules in Alzheimer disease. Proc Natl Acad Sci U S A **91**: 5562-5566, 1994
27) Alonso Adel C, Li B, Grundke-Iqbal I, Iqbal K: Polymerization of hyperphosphorylated tau into filaments eliminates its inhibitory activity. Proc Natl Acad Sci U S A **103**: 8864-8869, 2006
28) Morishima-Kawashima M, Hasegawa M, Takio K, Suzuki M, Yoshida H, et al: Proline-directed and non-proline-directed phosphorylation of PHF-tau. J Biol Chem **270**: 823-829, 1995
29) Drewes G, Ebneth A, Preuss U, Mandelkow EM, Mandelkow E: MARK, a novel family of protein kinases that phosphorylate microtubule-associated proteins and trigger microtubule disruption. Cell **89**: 297-308, 1997
30) Kishi M, Pan YA, Crump JG, Sanes JR: Mammalian SAD kinases are required for neuronal polarization. Science **307**: 929-932, 2005
31) Pei JJ, An WL, Zhou XW, Nishimura T, Norberg J, et al: P70 S6 kinase mediates tau phosphorylation and synthesis. FEBS Lett **580**: 107-114, 2006
32) Jeganathan S, von Bergen M, Brutlach H, Steinhoff HJ, Mandelkow E: Global hairpin folding of tau in solution. Biochemistry **45**: 2283-2293, 2006
33) Jeganathan S, Hascher A, Chinnathambi S, Biernat J, Mandelkow EM, et al: Proline-directed pseudophosphorylation at AT8 and PHF1 epitopes induces a compaction of the paperclip folding of Tau and generates a pathological (MC-1) conformation. J Biol Chem **283**: 32066-32076, 2008
34) Maeda S, Sahara N, Saito Y, Murayama M, Yoshiike Y, et al: Granular tau oligomers as intermediates of tau filaments. Biochemistry **46**: 3856-3861, 2007
35) Whiscick C, Bentham P, Wischick D, Seng KM: Tau aggregation inhibitor (TAI) therapy with RENBER arrests disease progression in mild and moderate Alzheimer's disease over 50 weeks. Alzheimer's & Dementia **4**: T167, 2008

doi:10.1016/j.jmb.2009.10.068 J. Mol. Biol. (2010) 395, 445–456

JMB

Available online at www.sciencedirect.com

ScienceDirect

ELSEVIER

Characterization of Inhibitor-Bound α-Synuclein Dimer: Role of α-Synuclein N-Terminal Region in Dimerization and Inhibitor Binding

Yoshiki Yamaguchi[1,2*†], Masami Masuda[3,4†], Hiroaki Sasakawa[1,5], Takashi Nonaka[3], Shinya Hanashima[2], Shin-ichi Hisanaga[4], Koichi Kato[1,5,6] and Masato Hasegawa[3*]

[1]*Department of Structural Biology and Biomolecular Engineering, Graduate School of Pharmaceutical Sciences, Nagoya City University, 3-1 Tanabe-dori, Mizuho-ku, Nagoya 467-8603, Japan*

[2]*Structural Glycobiology Team, Systems Glycobiology Research Group, Chemical Biology Department, RIKEN, Advanced Science Institute, 2-1 Hirosawa Wako, Saitama 351-0198, Japan*

[3]*Department of Molecular Neurobiology, Tokyo Institute of Psychiatry, 2-1-8 Kamikitazawa, Setagaya-ku, Tokyo 156-8585, Japan*

[4]*Molecular Neuroscience Laboratory, Graduate School of Science, Tokyo Metropolitan University, 1-1 Minami-Osawa, Hachioji-shi, Tokyo 192-0397, Japan*

[5]*Institute for Molecular Science, National Institutes of Natural Sciences, 5-1 Higashiyama, Myodaiji, Okazaki, Aichi 444-8787, Japan*

α-Synuclein is a major component of filamentous inclusions that are histological hallmarks of Parkinson's disease and other α-synucleinopathies. Previous analyses have revealed that several polyphenols inhibit α-synuclein assembly with low micromolar IC_{50} values, and that SDS-stable, noncytotoxic soluble α-synuclein oligomers are formed in their presence. Structural elucidation of inhibitor-bound α-synuclein oligomers is obviously required for the better understanding of the inhibitory mechanism. In order to characterize inhibitor-bound α-synucleins in detail, we have prepared α-synuclein dimers in the presence of polyphenol inhibitors, exifone, gossypetin, and dopamine, and purified the products. Peptide mapping and mass spectrometric analysis revealed that exifone-treated α-synuclein monomer and dimer were oxidized at all four methionine residues of α-synuclein. Immunoblot analysis and redox-cycling staining of endoproteinase Asp-N-digested products showed that the N-terminal region (1–60) is involved in the dimerization and exifone binding of α-synuclein. Ultra-high-field NMR analysis of inhibitor-bound α-synuclein dimers showed that the signals derived from the N-terminal region of α-synuclein exhibited line broadening, confirming that the N-terminal region is involved in inhibitor-induced dimerization. The C-terminal portion still predominantly exhibited the random-coil character observed in monomeric α-synuclein. We propose that the N-terminal region of α-synuclein plays a key role in the formation of α-synuclein assemblies.

*Corresponding authors. Y. Yamaguchi is to be contacted at Structural Glycobiology Team, Systems Glycobiology Research Group, Chemical Biology Department, RIKEN, Advanced Science Institute, 2-1 Hirosawa Wako, Saitama 351-0198, Japan. E-mail addresses: yyoshiki@riken.jp; masato@prit.go.jp.

† Y.Y. and M.M. contributed equally to this work.

Abbreviations used: PD, Parkinson's disease; Exi-monomer, exifone-bound monomer; Exi-dimer, exifone-bound dimer; HSQC, heteronuclear single quantum coherence; NBT, nitroblue tetrazolium; MALDI-TOF, matrix-assisted laser desorption/ionization time-of-flight; MS, mass spectrometry.

0022-2836/$ - see front matter © 2009 Elsevier Ltd. All rights reserved.

[6]*Okazaki Institute for Integrative Bioscience, National Institutes of Natural Sciences, 5-1 Higashiyama, Myodaiji, Okazaki, Aichi 444-8787, Japan*

Received 3 April 2009; received in revised form 26 September 2009; accepted 27 October 2009
Available online 3 November 2009

Edited by S. Radford

Keywords: NMR; α-synuclein; dimer; dopamine; Parkinson's disease

Introduction

Parkinson's disease (PD) and other α-synucleinopathies are progressive neurodegenerative diseases characterized by the selective loss of dopaminergic neurons and deposition of filamentous Lewy bodies, of which α-synuclein is the major component. Formation of amyloid fibrils and/or intermediate oligomers of α-synuclein is a complex process, and small-molecular inhibitors have been used to investigate the pathways involved. Conway *et al.* reported that catechol-containing compounds, including dopamine, inhibited the formation of α-synuclein fibrils, causing the accumulation of α-synuclein protofibrils.[1] It was also reported that α-synuclein fibrillization was inhibited by dopamine analogues, and α-synuclein oligomers were stabilized by these compounds.[2] We have previously reported that several polyphenols inhibited α-synuclein assembly with IC_{50} values in the low micromolar range, and that noncytotoxic, SDS-stable α-synuclein oligomers were formed in the presence of inhibitory compounds.[3]

Analyses of the interactions between small-molecular inhibitory compounds and α-synuclein have been reported by many groups, but the mechanisms involved remain controversial. It was proposed that amyloid fibril formation is inhibited by polyphenol compounds *via* noncovalent aromatic interactions with the amyloidogenic core.[4] A recent report showed that chemical aggregates inhibited amyloid formation of the yeast and mouse prion proteins in a manner characteristic of colloidal inhibition, suggesting a nonspecific mechanism.[5] Mutagenesis and competition studies with specific synthetic peptides suggested α-synuclein residues 125–129 (YEMPS) as an important region for dopamine-induced inhibition of α-synuclein fibrillization, and the inhibition was proposed to be due to conformational alterations of α-synuclein induced by noncovalent interaction with oxidized dopamine.[6] Molecular dynamics simulations suggest that dopamine binds to the YEMPS region, and the bound dopamine is further stabilized by long-range electrostatic interactions with E83 in the NAC region.[7] A recent NMR analysis indicated that a polyphenol compound, epigallocatechin gallate, noncovalently binds to the C-terminal region of α-synuclein (D119, S129, E130, and D135).[8] NMR analysis showed that A53T mutant α-synuclein, which is linked to autosomal dominant forms of PD, has a greater propensity to aggregate in the presence of dopamine, compared to wild-type α-synuclein.[9] Meanwhile, NMR characterization of the interaction between α-synuclein and various small molecules indicated that residues 3–18 and 38–51 act as noncovalent binding sites for inhibitory compounds.[10]

Covalent attachment of inhibitors to α-synuclein, on the other hand, has been proposed by several groups. Conway *et al.* suggested that 5–10% of dopamine was covalently incorporated into α-synuclein by radical coupling (dopamine-derived orthoquinone to Tyr) and/or nucleophilic attack (e.g., Lys forming a Schiff base with the orthoquinene).[1] Mass spectrometry (MS) and NMR characterization suggested that the oxidation product (quinones) of a dopamine analogue was covalently linked to the amino groups of the α-synuclein chain, thereby generating α-synuclein–quinone adducts.[2] Thus, the binding mode and binding site(s) of small-molecular inhibitors remain controversial.

The conformation of inhibitor-induced α-synuclein oligomers is also a matter of debate. Norris *et al.* reported that spherical oligomers of dopamine-modified α-synuclein take a predominantly random-coil structure with some β-pleated sheets on the basis of CD and Fourier-transform infrared spectroscopy studies.[6] Another group demonstrated that in the presence of small inhibitory molecules, α-synuclein is still dominated by random-coil character.[10] Ehrnhoefer *et al.* proposed that epigallocatechin prevented the conversion of monomeric α-synuclein into toxic on-pathway aggregation intermediates and resulted in the formation of unstructured, nontoxic α-synuclein oligomers that they considered to be off-pathway.[8] On the other hand, it has recently been reported that a flavonoid, baicalein, stabilized β-sheet-enriched oligomers based on CD and Fourier-transform infrared spectroscopy analysis.[11] The baicalein-stabilized oligomers were characterized as quite compact globular species based on small-angle X-ray scattering data and atomic force microscopy.

Masuda *et al.* isolated α-synuclein dimers formed in the presence of inhibitory compounds,[3] and the isolated soluble dimers were recently characterized using a panel of epitope-specific α-synuclein antibodies.[12] The reactivities of the antibodies indicated that the conformations of polyphenol-bound α-synuclein dimers differ from those of unbound monomers, but resemble those of amyloid fibrils, suggesting that inhibitor-bound molecular species are on-pathway intermediates.

This situation prompted us to carry out a comprehensive analysis of inhibitor-treated α-synucleins by means of NMR spectroscopy in conjunction with other biochemical methods, such as peptide mapping, immunoblotting, and redox-cycling staining. We have previously analyzed the antibody binding and site-specific phosphorylation of α-synuclein using ultra-high-field NMR spectroscopy.[13] For the structural characterization, we prepared and purified a ^{15}N-labeled α-synuclein dimer in the presence of polyphenol inhibitors on a milligram scale and analyzed it by ultra-high-field NMR spectroscopy recorded at a proton observation frequency of 920 MHz.

Results and Discussion

Isolation and characterization of inhibitor-bound α-synuclein dimer and monomer

SDS-stable, noncytotoxic α-synuclein oligomers were detected in the soluble fraction in the presence of inhibitory compounds such as polyphenols.[3] For detailed characterization of inhibitor-induced α-synuclein oligomers, we attempted to prepare exifone-, gossypetin-, and dopamine-induced α-synuclein dimer and monomer (for inhibitor structures, see Fig. 1) and to separate them by gel-filtration chromatography as described.[12] Fig. 2a shows the HPLC patterns of control and exifone-treated α-synucleins. The HPLC fractions of exifone-treated α-synuclein were analyzed by SDS-PAGE and Western blotting (Fig. 2b). The data indicate that the exifone-treated α-synuclein dimer (Exi-dimer) was successfully purified by gel-filtration chromatography. The homogeneity of inhibitor-induced monomer and dimer was also checked by diffusion NMR experiments (data not shown). α-Synuclein monomer and dimer treated with exifone, as well as control monomer (without inhibitor), were subjected to matrix-assisted laser desorption/ionization time-of-flight (MALDI-TOF) MS measurements (Fig. 2c). α-Synuclein monomer (control) showed a major signal at 14,460 Da, which matched the predicted mass (14,460 Da). On the other hand, exifone-treated monomer (Exi-monomer) gave a major signal at 14,524 Da, which corresponded to that of α-synuclein plus 64 Da. Exifone-bound α-synuclein (molecular mass of exifone, 278.2 Da) was not detected, presumably because exifone binding was noncovalent. The MS spectrum of Exi-dimer showed a broad peak at around 30 kDa and 15 kDa, and we could not obtain an accurate molecular mass. The peak at 15 kDa might be the doubly charged ion of the Exi-dimer and/or the monomer released from the Exi-dimer in the ionization process. To estimate the ratio of exifone bound to α-synuclein dimer and monomer, absorption of exifone at 385 nm was measured for Exi-dimer and Exi-monomer. The results indicate that Exi-dimer contains around 3 molecules of exifone per α-synuclein monomer, while Exi-monomer

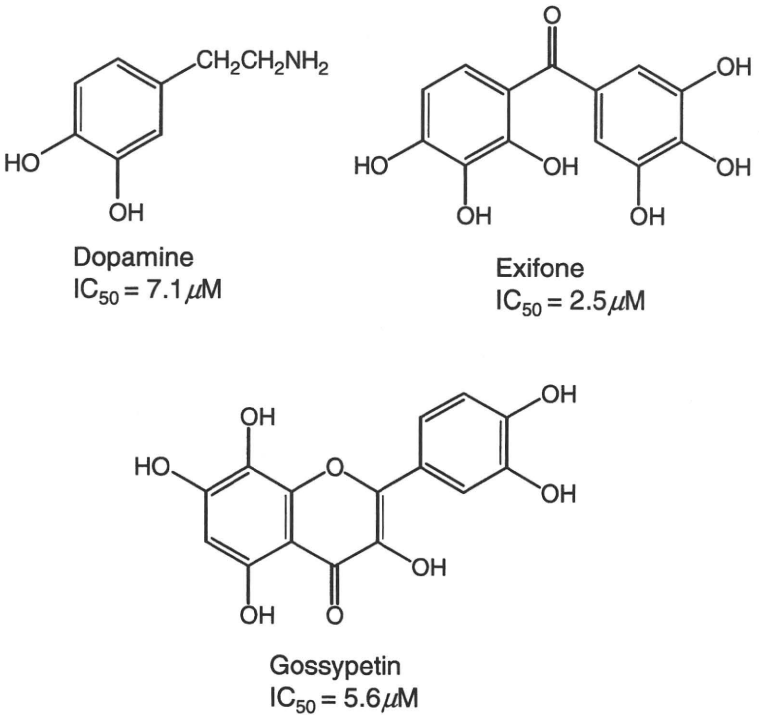

Fig. 1. Chemical structures of dopamine, exifone, and gossypetin with their IC_{50} values for inhibition of α-synuclein filament assembly.[3]

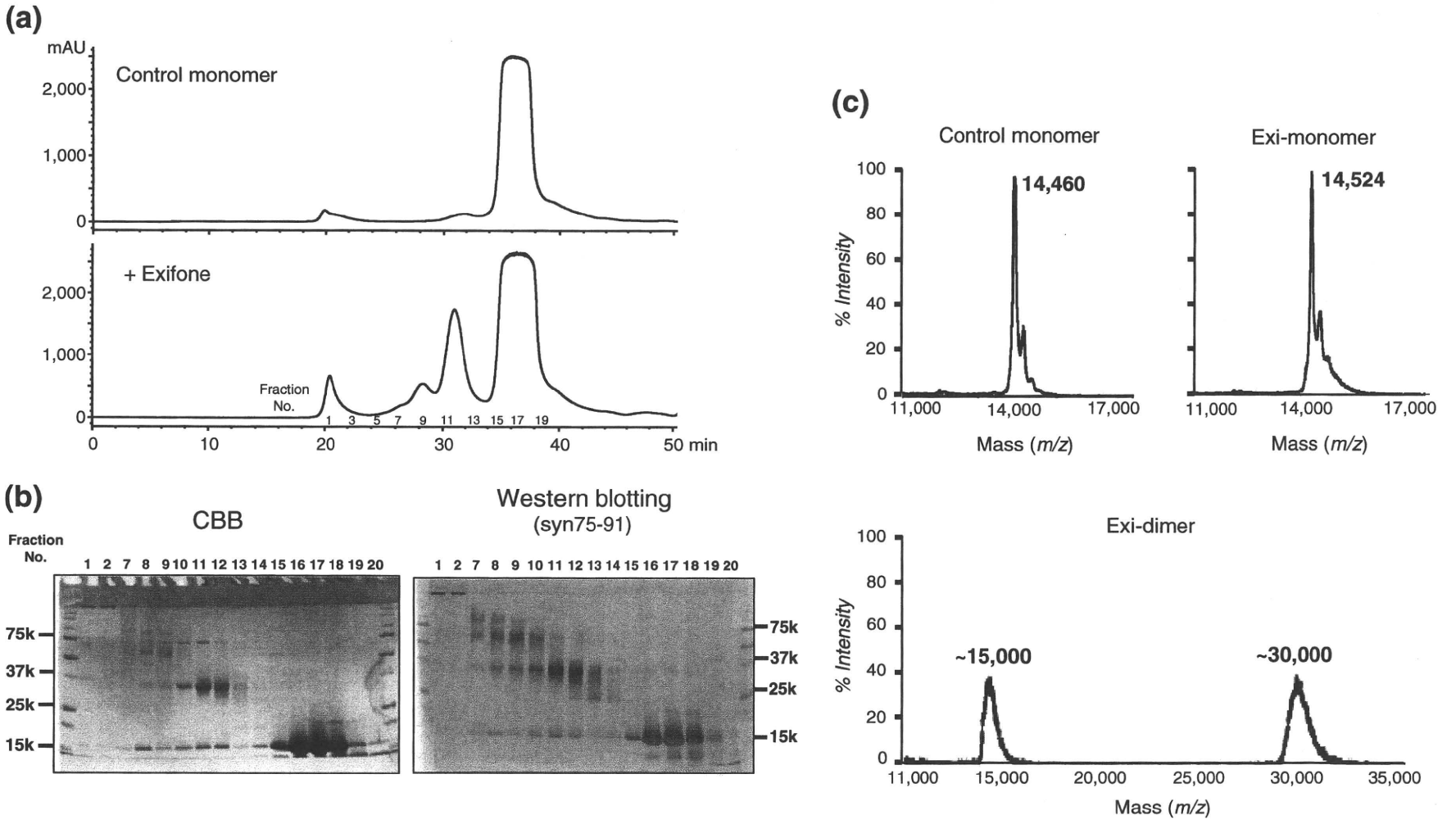

Fig. 2. Isolation and characterization of exifone-bound α-synucleins. (a) Separation of exifone-treated α-synuclein monomer and dimer by gel-filtration chromatography (detection: absorbance at 214 nm). (b) SDS-PAGE of fractions separated by gel-filtration chromatography (Coomassie brilliant blue staining and Western blotting). Pooled fractions 11–12 and 16–18 were used as Exi-dimer and Exi-monomer, respectively. (c) Partial MALDI-TOF MS spectra of α-synuclein monomer (control), Exi-monomer, and Exi-dimer.

contains one exifone molecule per α-synuclein chain (Supplementary Fig. S1).

For the identification of the modification (corresponding to a molecular mass of 64 Da) found in the Exi-monomer, α-synuclein was incubated with various concentrations of exifone (0, 0.2, 0.5, 1, and 2 mM) and the resulting samples were analyzed by MS (Supplementary Fig. S2). The molecular mass of α-synuclein increased in an exifone concentration-dependent manner and reached 14,528 Da (Supplementary Fig. S2a and b). A similar increase in molecular mass was reported in the presence of H_2O_2, which oxidized methionine residues to methionine sulfoxide.[14] Methionine oxidation is known to increase mass by 16 Da. α-Synuclein has four methionine residues, Met1, Met5, Met116, and Met127, and thus the oxidation of all the methionine residues would result in an increase in mass of 64 Da (Supplementary Fig. S3c). Indeed, α-synuclein incubated with various concentrations of H_2O_2 showed a concentration-dependent increase in molecular mass of up to 14,533 Da (Supplementary Fig. S3a and b), similar to that seen in the case of exifone. These results strongly suggest that all the methionine residues of Exi-monomer were oxidized to methionine sulfoxide.

Peptide mapping of inhibitor-induced α-synuclein dimer and monomer

In order to confirm the oxidation of methionine, control α-synuclein, Exi-monomer, Exi-dimer, and H_2O_2-treated α-synuclein monomer were digested with trypsin, and the resulting peptide mixtures were analyzed by reverse-phase HPLC (Fig. 3a). The elution patterns of peptides derived from Exi-monomer and Exi-dimer exhibited different profiles compared with that of control α-synuclein. Peaks 5 and 10 in the map of control α-synuclein were absent in the maps of Exi-monomer and Exi-dimer. Instead, peaks 11–18 newly appeared in the maps of Exi-monomer and Exi-dimer. The patterns of Exi-monomer and Exi-dimer were similar to those of α-synuclein oxidized with H_2O_2. All the peaks were analyzed by MS and the results are summarized in Fig. 3b. Peaks 5 and 10 were identified as Met1–Lys6 (containing two methionines, Met1 and Met5) and Asn103–Ala140 (containing Met116 and Met127), respectively. In the case of Exi-monomer or Exi-dimer, peaks 11, 15, and 19 were identified as Met1–Lys6 including two oxidized methionines. Peaks 12, 16, and 20 were identified as Asn103–Ala140 including oxidized Met116 and Met127. Peaks 13, 14, 16, and 17 were derived from Asn103–Ala140 oxidized at either Met116 or Met127. Similar results were obtained for dopamine-bound dimer and monomer (data not shown). These results clearly indicate that the inhibitors exifone and dopamine have the ability to oxidize methionine residues on α-synuclein. It is established that α-synuclein assembly was inhibited by exifone at low micromolar range (IC_{50}=2.5 μM),[3] and methionine sulfoxide could not be detected at a low concentration of exifone (data not shown). These findings suggest that the stabilization of intermediate oligomers by small molecules is responsible for the inhibition of filament formation, and oxidation of methionine does not seem to play a major role in inhibition.

No covalent inhibitor–peptide adducts or cross-linked peptides were detected in the peptide mapping experiments, indicating that the inhibitors bind noncovalently to α-synuclein and that α-synuclein dimer is formed in a noncovalent fashion. These observations are consistent with the results of MALDI MS analysis of Exi-monomer, which showed no inhibitor adducts (Fig. 2c). Our extensive liquid chromatography–electrospray ionization MS analysis also did not show the covalent inhibitor adducts or α-synuclein dimer (data not shown). Further, more detailed biochemical studies to investigate the modes of inhibitor binding and dimerization are currently in progress.

Characterization of exifone-binding regions in α-synuclein

Exifone is an antioxidant and thus can be detected by redox-cycling staining, which is a well-established method for detecting quinoproteins.[15] As expected, Exi-dimer and Exi-monomer were stained as purple bands by redox-cycling staining due to nitroblue tetrazolium (NBT) reduction to formazan (Fig. 4a), while untreated control α-synuclein showed no staining. This result shows that redox-cycling staining is useful for examining the exifone-binding regions in α-synuclein. In order to determine the binding region of exifone and the regions involved in the dimerization, Exi-dimer was digested with endoproteinase Asp-N and the resulting peptides were detected with silver or redox-cycling staining. Asp-N digestion of Exi-dimer gave two major fragments, corresponding to molecular masses of 20 kDa (no. 1) and 16 kDa (no. 2), on SDS-PAGE after silver staining (Fig. 4b). These two bands were positive for redox-cycling staining. Since α-synuclein monomer migrates at 15 kDa, these fragments represent dimeric peptides stabilized by exifone. α-Synuclein has six aspartic acid residues (Asp2, Asp98, Asp115, Asp119, Asp121, and Asp135). Immunoblot analysis with a panel of site-specific anti-α-synuclein antibodies (Fig. 5) suggested that the 20-kDa fragment contains the dimerized N-terminal fragment Met1–Met97 of α-synuclein (cleaved at the N-terminus of Asp98). The 16-kDa fragment was also labeled with antibodies to the N-terminal and central portions of α-synuclein (residues 1–50). It has been reported that Asp-N cleaves peptide bonds N-terminal to glutamate as well as aspartate residues.[16,17] Glu57 and/or Glu61 are found in the middle of α-synuclein and are candidate Asp-N cleavage sites to produce the 16-kDa fragment. The reactivity of anti-α-synuclein antibodies and the relaxed specificity of Asp-N indicate that the 16-kDa fragment corresponds to a dimer composed of Met1–Ala56/Lys60. These results suggest that the N-terminal region (1–60) of α-synuclein is involved in

the dimerization and exifone binding. This is in contrast with a previous report by Norris *et al.*, in which they suggested that dopamine inhibited the aggregation of α-synuclein by binding to the C-terminal residues 125–129 (i.e., YEMPS) and stabilizing the soluble oligomers.[6] The discrepancy might be due to the fact that they analyzed the dopamine-binding sites by using deletion mutants lacking the C-terminal regions and did not use full-length α-synucleins.

High-resolution NMR spectra of inhibitor-bound α-synuclein monomer and dimer

In order to characterize the behavior of α-synuclein monomer and dimer formed in the presence of polyphenolic compounds, we conducted a structural analysis of inhibitor-bound α-synuclein monomer and dimer using ultra-high-field NMR spectroscopy. NMR signals of backbone amides constitute excellent probes to provide maps of the interacting sites and to examine the effects of modifications.[13] Fig. 6a and b shows the $^{1}H-^{15}N$ heteronuclear single quantum coherence (HSQC) spectra of uniformly ^{15}N-labeled Exi-monomer and Exi-dimer, as well as control monomer, recorded at a proton observation frequency of 920 MHz. The amide resonances of Exi-monomer and Exi-dimer were assigned by comparing the NMR spectral data with those of control α-synuclein monomer. Little chemical shift difference was detected between Exi-monomer and control monomer for most observed peaks, except for the signals corresponding

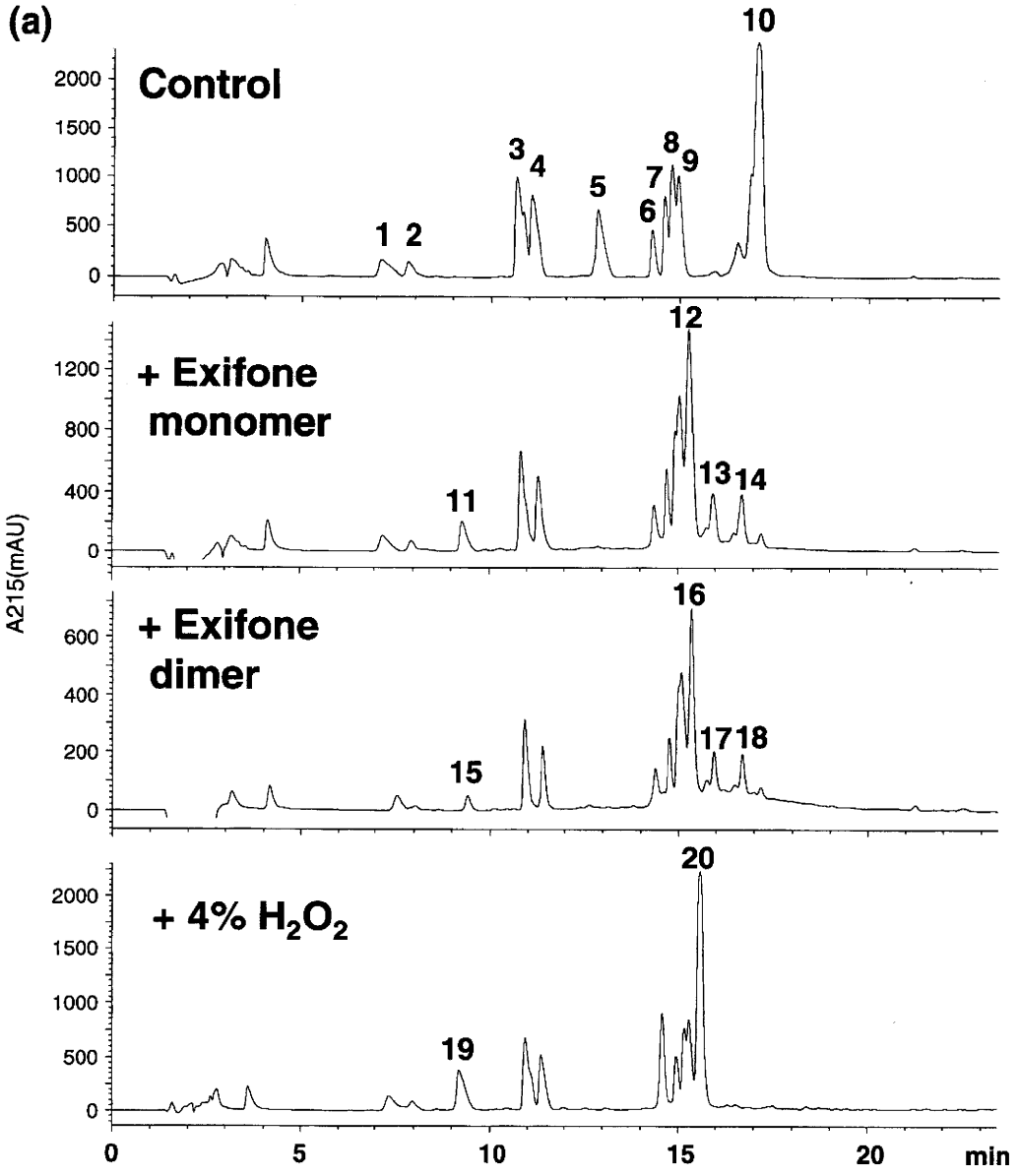

Fig. 3. Tryptic peptide mapping and MS analysis of α-synucleins. (a) Reverse-phase HPLC patterns of monomeric α-synuclein (control), Exi-monomer, Exi-dimer, and H_2O_2-treated α-synuclein monomer. (b) Observed masses and peak assignments of the peptides separated on a reverse-phase column. Oxidation of methionine residues was observed in Exi-monomer and Exi-dimer, as well as H_2O_2-treated α-synuclein monomer.

(b)

Peak No.	$(M+H)^+$ Observed	$(M+H)^+$ Calculated	Assignment
1	830.6 873.5 1072.6	830.4 873.4 1072.5	QGVAEAAGK (24-32) EGVVAAAEK (13-21) AKEGVVAAAEK (11-21)
2	1180.7 1295.8 1524.8	1180.6 1295.6 1524.8	TKEGVLYVGSK (33-43) EGVVHGVATVAEK (46-58) TKEGVVHGVATVAEK (44-58)
3	951.5	951.5	EGVLYVGSK (35-43)
4	1295.7	1295.6	EGVVHGVATVAEK (46-58)
5	770.5	770.3	MDVFMK (1-6)
6	1606.6	1606.8	TVEGAGSIAAATGFVKK (81-97)
7	2157.2	2157.1	TKEQVTNVGGAVVTGVTAVAQK (58-80)
8	1478.5	1478.7	TVEGAGSIAAATGFVK (81-96)
9	1928.0	1928.0	EQVTNVGGAVVTGVTAVAQK (61-80)
10	4295.0	4286.7	NEEGAPQEGILEDMPVDPDNAYEMPSEEGYQDYEPEA (103-140)
11	803.0	802.3.0	M*DVFM*K (1-6) (M*:methionine sulfoxide)
12	4322.0	4318.7	NEEGAPQEGILEDM*PVDPDNAYEM*PSEEGYQDYEPEA (103-140)
13	4311.0	4302.7	NEEGAPQEGILEDM#PVDPDNAYEM#PSEEGYQDYEPEA (103-140) (One of two methionine residues (M#) was oxidized)
14	4312.0	4302.7	NEEGAPQEGILEDM#PVDPDNAYEM#PSEEGYQDYEPEA (103-140)
15	802.0	802.3	M*DVFM*K (1-6)
16	4322.0	4318.7	NEEGAPQEGILEDM*PVDPDNAYEM*PSEEGYQDYEPEA (103-140)
17	4311.0	4302.7	NEEGAPQEGILEDM#PVDPDNAYEM#PSEEGYQDYEPEA (103-140)
18	4312.0	4302.7	NEEGAPQEGILEDM#PVDPDNAYEM#PSEEGYQDYEPEA (103-140)
19	803.0	802.3	M*DVFM*K (1-6)
20	4322.0	4318.7	NEEGAPQEGILEDM*PVDPDNAYEM*PSEEGYQDYEPEA (103-140)

Fig. 3 *(legend on previous page)*

to Met5, Met116, Met127, and their neighboring residues (Fig 6a). The observed chemical shift differences are mostly attributable to the oxidation of methionine residues. The differences in peak intensities between Exi-monomer and control monomer were also generally small (Fig. 6c). These results indicate that the dynamical features of both synuclein monomers are almost the same, and methionine oxidation itself does not greatly influence the structural characteristics of α-synuclein.

It is noteworthy that significant reductions in signal intensity [I(Exi-dimer)/I(control monomer)< 0.8] were observed for the peaks originating from the N-terminal region (1–60) of Exi-dimer compared with the control monomer (Fig. 6d). This result shows that the N-terminal regions are involved in exifone-induced dimerization of α-synuclein, in accordance with the results obtained from Asp-N digestion of the Exi-dimer. The gradual reduction in the signal intensities might be explained by heterogeneous dimerization around the N-terminus. The observed reduction in signal intensity, in our case, was not due to chemical exchange between the inhibitor-free and inhibitor-bound states of α-synuclein, as had been suggested by Rao *et al.*,[10] because the inhibitor-induced dimer and monomer were each purified to homogeneity and free or exchangeable inhibitors were removed by gel-filtration column chromatography and buffer exchange. Similar NMR spectra were observed for dopamine- and gossypetin-induced dimers (Supplementary Fig. S4), indicating that the N-terminal dimerization modes induced by dopamine, exifone, and gossypetin are the same or at least very similar. On the other hand, the C-terminal portion of exifone-bound dimer was still predominantly random coil in character, as observed in the control monomeric α-synuclein. These

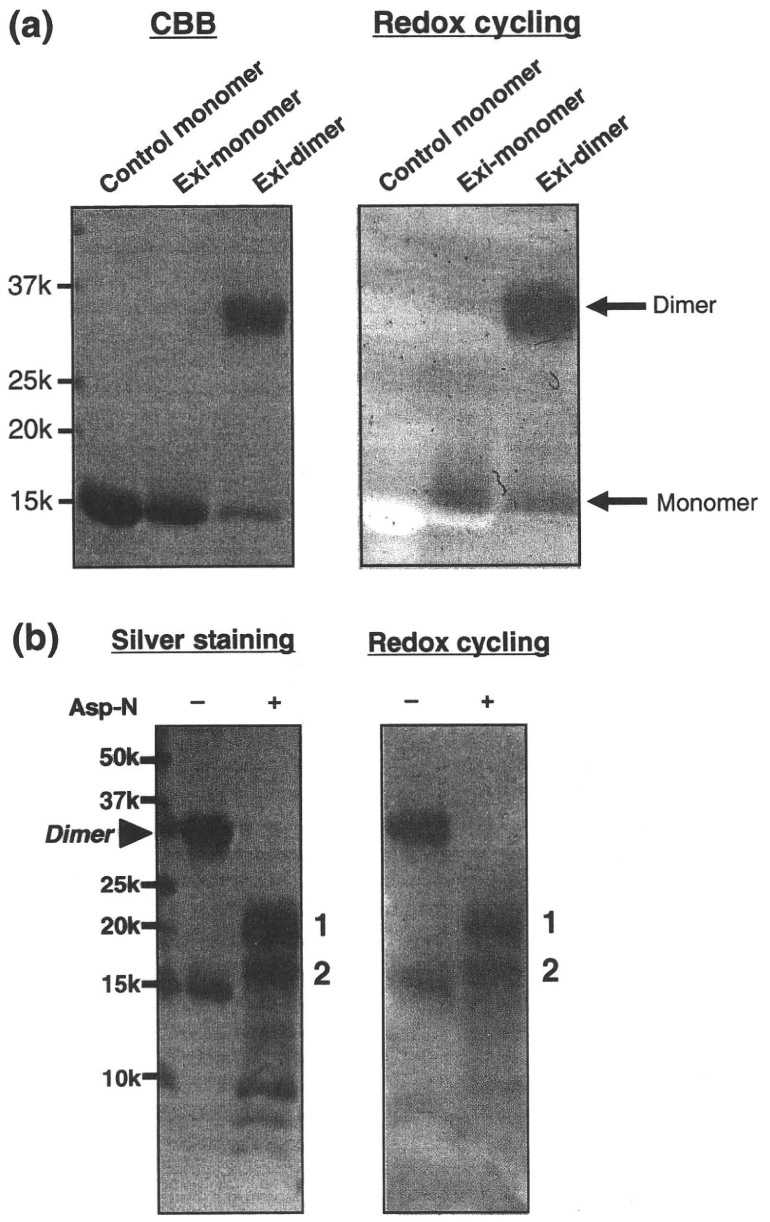

Fig. 4. Detection of exifone bound to α-synucleins by redox-cycling staining. (a) Control monomer, Exi-monomer, and Exi-dimer were stained with Coomassie brilliant blue (left) or by redox cycling (right). Exifone-bound α-synucleins were stained by redox cycling, appearing as purple-blue bands in the Exi-monomer and Exi-dimer lanes, due to NBT reduction to formazan (right). (b) Asp-N digestion of Exi-dimer. Exi-dimer was digested with endoproteinase Asp-N and the fragments were detected by silver staining (left) and redox staining (right). Two major bands corresponding to 20 kDa and 16 kDa (nos. 1 and 2, respectively) were positive for redox-cycling staining.

observations indicate the importance of the N-terminal region in α-synuclein assembly.

It is of note that three missense mutations in familial PD (A30P, E46K, and A53T) are located in the N-terminal region of α-synuclein. Recent NMR analyses suggest that these mutations may be altering the physicochemical properties of the protein, such as net charge (E46K) and secondary-structure propensity (A30P and A53T).[19] The binding of exifone, gossypetin, or dopamine to α-synuclein might also alter the net charge and/or secondary-structure propensity.

We did not observe the colloidal formation of exifone, gossypetin, or dopamine by electron microscopy (data not shown) as reported by Feng *et al.*[5] The discrepancy might be due to differences in the compounds used or differences in the proteins investigated. The inhibition mechanism of these three compounds seems rather specific because the N-terminal region was specifically involved in inhibitor binding, which is in contrast to the nonspecific colloidal inhibition.

In summary, we have characterized the inhibitor-bound α-synuclein dimer and showed that the N-terminal region (1–60) plays a key role in dimerization and inhibitor binding. Further studies are under way in our laboratory to elucidate the mechanisms of inhibitor-induced oligomer formation at atomic resolution.

Materials and Methods

Antibodies

Polyclonal antibodies were raised against synthetic peptides corresponding to residues 1–10, 11–20, 21–30, 31–40, 41–50, 51–60, 61–70, 75–91, and 131–140 of human α-synucleins, prepared as described previously.[12] Antibody

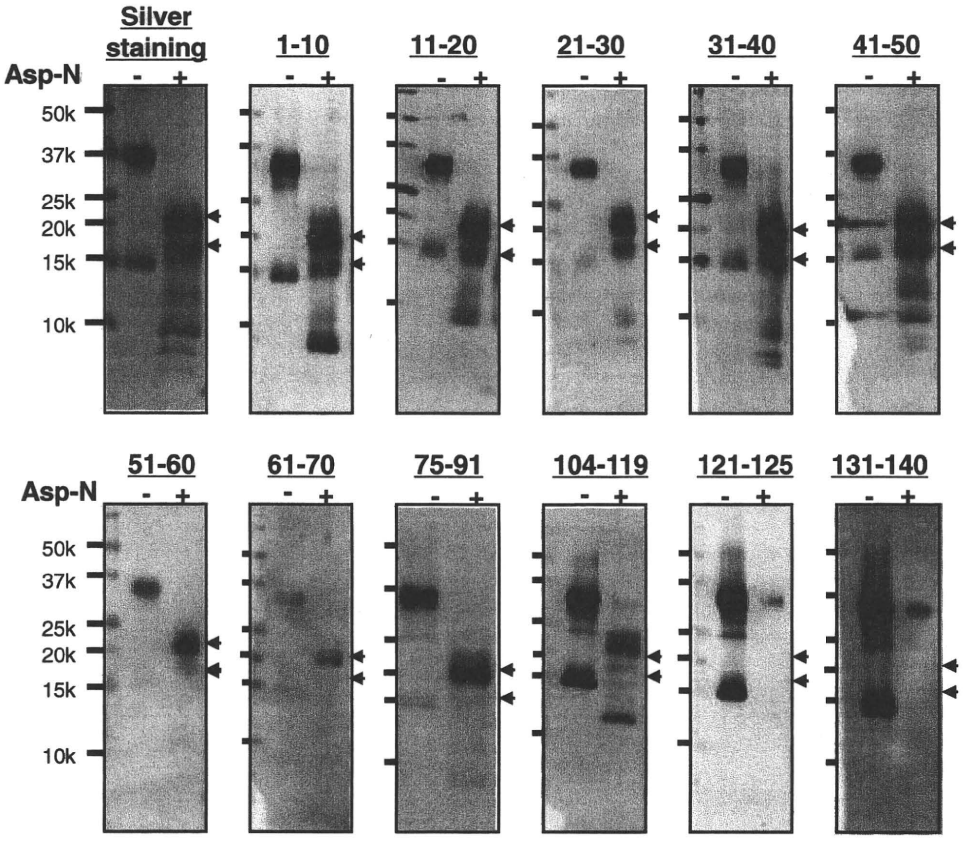

Fig. 5. Immunoblot analysis of Asp-N digests of Exi-dimer. Silver staining and immunoblots of Asp-N digests of Exi-dimer with a panel of anti-α-synuclein antibodies raised against nine peptides (corresponding to residues 1–10, 11–20, 21–30, 31–40, 41–50, 51–60, 61–70, 75–91, and 131–140).[12] Experimental details are given in Materials and Methods. Two major fragments (band nos. 1 and 2) were detected with silver staining (indicated with arrowheads). Fragment no. 1 was positive for antibodies to the N-terminal region, 1–97, and no. 2 was positive for antibodies to the N-terminal region, 1–50.

Syn259, which recognizes residues 104–119 of α-synuclein, was kindly provided by Dr. S. Nakajo. Monoclonal antibody Syn211, which recognizes residues 121–125 of α-synuclein, was purchased from Zymed.

Protein expression and purification

Expression of isotopically labeled α-synuclein was performed as described.[13] Human α-synuclein cDNA in bacterial expression plasmid pRK172 was used for production of isotopically labeled protein for NMR analyses.[20] Codon 136 was changed from TAC to TAT by site-directed mutagenesis to avoid cysteine misincorporation.[21] Uniformly ^{15}N-labeled α-synuclein was expressed in *Escherichia coli* BL21(DE3) cells grown in M9 minimal medium containing 1 g/L [^{15}N]NH_4Cl, while unlabeled α-synuclein was expressed using LB medium. Cell lysates were subjected to boiling and subsequently to ammonium sulfate precipitation. The precipitated α-synuclein was extensively dialyzed against 20 mM Tris–HCl (pH 8.0) and then purified with DEAE ion-exchange chromatography.

Preparation of inhibitor-bound α-synuclein monomers and dimers

Purified ^{15}N-labeled recombinant α-synuclein (9 mg/mL) was incubated with 2 mM inhibitor (exifone, gossypetin, or dopamine; see Fig. 1) for 30 days at 37 °C in 30 mM Tris–HCl containing 0.1% sodium azide. The samples were then centrifuged at 113,000*g* for 20 min. The supernatants were loaded on a Sephadex G-25 gel-filtration column to separate oligomers from unbound inhibitor. The eluates were fractionated on a Superdex 200 gel-filtration column (1 cm×30 cm), eluted with 10 mM Tris–HCl (pH 7.5) containing 150 mM NaCl. Eluates were monitored at 215 nm. α-Synuclein monomer and dimer fractions were each concentrated and the concentrates were subjected to NMR analysis. Protein concentrations were determined using HPLC and bicinchoninic acid protein assay kit (Pierce).

Mass spectrometry

Samples were spotted on a sample plate and mixed with the matrix solutions, saturated sinapic acid (Fluka) or α-cyano-4-hydroxycinnamic acid (Fluka) in 50% acetonitrile/H_2O containing 0.1% (v/v) trifluoroacetic acid. Mass spectra were obtained by MALDI-TOF MS using a Voyager-DE Pro mass spectrometer (PerSeptive Biosystems).

Peptide mapping of H_2O_2-treated and inhibitor-bound α-synucleins

Inhibitor-bound α-synuclein monomer and dimer were prepared as described above. For methionine oxidation, α-synuclein monomer (7 mg/mL) was incubated with 0–4% H_2O_2 at room temperature for 20 min and then dialyzed

against 30 mM Tris–HCl (pH 7.5) to remove H_2O_2. To identify the modification, inhibitor-bound α-synuclein monomer and dimer, as well as H_2O_2-treated α-synuclein, were incubated with trypsin at 37 °C for 18 h at an enzyme-to-substrate ratio of 1:50 (mol/mol) in 30 mM Tris–HCl (pH 7.5). Digested peptide products were separated by reverse-phase HPLC on a Supersphere Select B column (2.1 × 125 mm; Merck) and analyzed by MALDI-TOF MS.

Determination of stoichiometry of exifone/α-synuclein complexes

The stoichiometry of exifone/α-synuclein complexes was determined by measuring the absorbance of exifone at 385 nm using a spectrophotometer (UV-1600 PC, Shimadzu Co). Exifone-bound monomeric and dimeric α-synucleins were isolated by gel-filtration chromatography as described above.

Redox-cycle staining

Samples were subjected to SDS-PAGE and transferred onto polyvinylidene fluoride membranes. The membranes were incubated in 0.24 mM NBT (Sigma), 2 M potassium glycinate solution (pH 10.0) in the dark for 16 h at room temperature and then dipped in 100 mM sodium borate (pH 10.0). Exifone-bound α-synuclein was specifically stained as purple-blue bands due to NBT reduction to formazan.

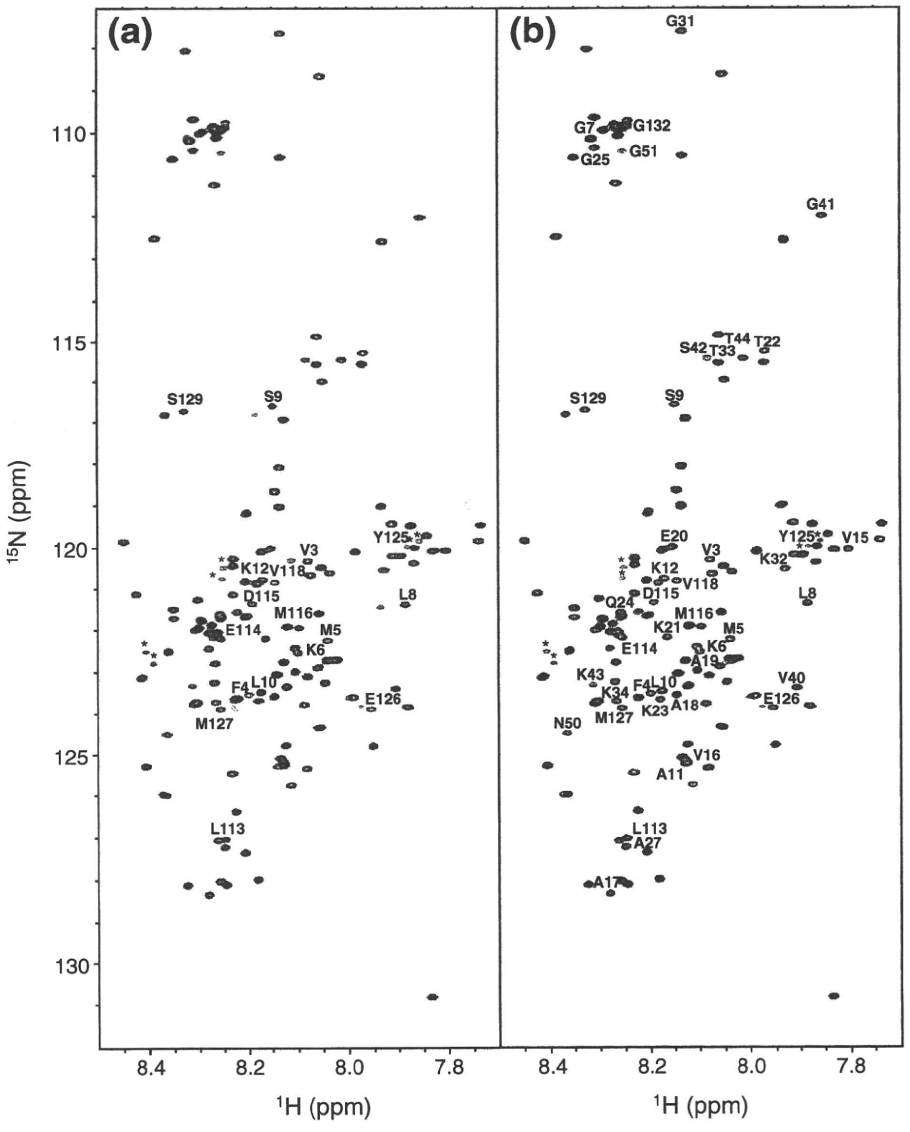

Fig. 6. NMR spectral comparison of exifone-bound ^{15}N-labeled α-synuclein dimer and control monomer. (a) ^{1}H–^{15}N HSQC spectra of ^{15}N-labeled Exi-monomer (red) and ^{15}N-labeled control monomer (black) recorded at a proton frequency of 920 MHz. (b) ^{1}H–^{15}N HSQC spectra of ^{15}N-labeled Exi-dimer (red) and ^{15}N-labeled control monomer (black). (c) Plot of the relative peak intensities, *I*(Exi-monomer)/*I*(monomer), of the HSQC cross-peaks in the Exi-monomer and control monomer *versus* the amino acid sequence of α-synuclein. (d) *I*(Exi-dimer)/*I*(monomer) of the HSQC cross-peaks in the Exi-dimer and control monomer. Signals derived from oxidized methionines and their neighboring residues (indicated with asterisks in a and b) were split and not taken into account. The peak splittings mostly reflect a mixture of *R* and *S* isomers of methionine sulfoxide.[18]

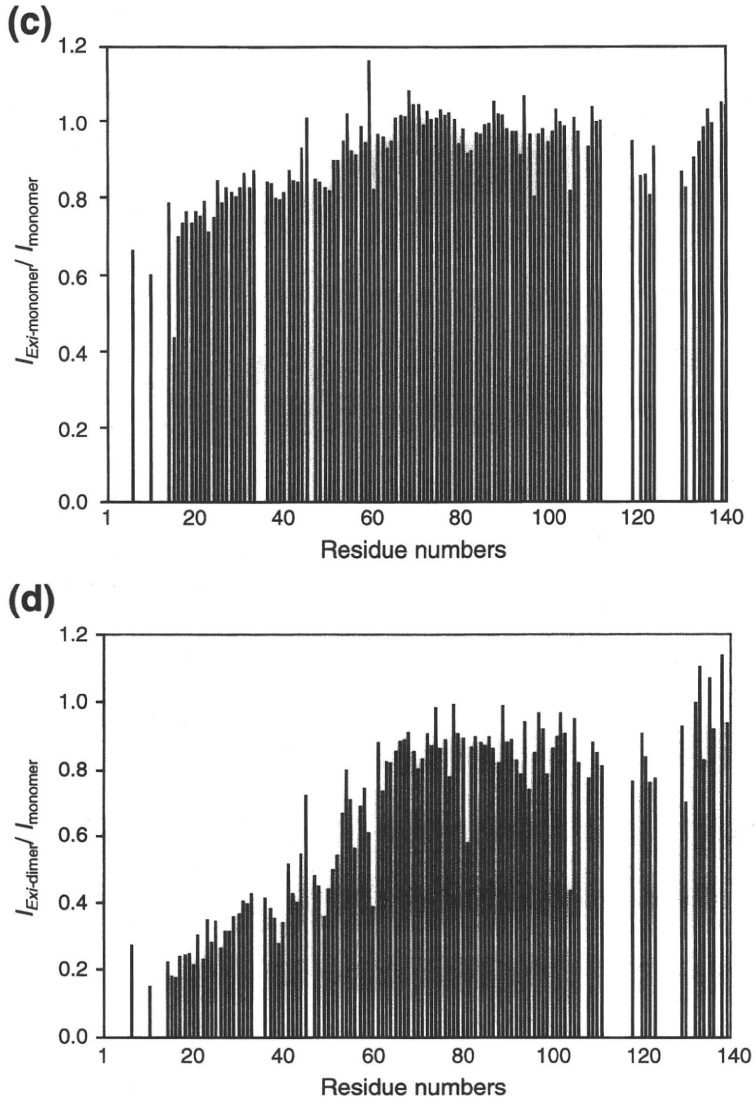

Fig. 6 *(legend on previous page)*

Asp-N digestion of α-synuclein dimer

α-Synuclein dimer (0.25 mg/mL) in 30 mM Tris–HCl (pH 7.5) was treated with 40 μg/mL of Asp-N (Roche) at 37 °C for 1 h. The reaction was stopped by adding 2× SDS sample buffer [4% SDS, 0.16 M Tris–HCl (pH 6.8), 30% glycerol] and the solution was boiled for 5 min. The samples were loaded onto 15% Tris/tricine SDS-PAGE gel, and the digested products were detected by silver staining (kit from Wako), immunoblotting, and redox-cycling staining. For immunoblotting, SDS-PAGE gels were blotted onto polyvinylidene fluoride membranes, blocked with 3% gelatin/phosphate-buffered saline, and incubated overnight at room temperature with anti-α-synuclein antibody in 10% FBS/phosphate-buffered saline. After washing, the blots were incubated for 2 h at room temperature with biotinylated secondary antibody (1:500) (Vector Laboratories). Following further washing, the blots were incubated with peroxidase-labeled avidin–biotin (Vector laboratories) for 30 min at room temperature and developed with $NiCl_2$-enhanced diaminobenzidine (Sigma).

NMR measurements

The samples for NMR experiments were prepared at a concentration of 0.1–1.0 mM in 90% H_2O/10% D_2O (v/v), 10 mM sodium phosphate buffer, and 100 mM NaCl at pH 7.0. NMR experiments were performed at 10 °C using a JEOL JNM-ECA920 spectrometer equipped with a 5-mm triple resonance probe. Backbone assignments of α-synuclein monomer were achieved by means of standard triple resonance experiments, as described previously.[13] The samples were checked by SDS-PAGE before and after NMR measurements, and it was confirmed that aggregation of inhibitor-bound α-synuclein monomer and dimer did not occur under these conditions. NMR time domain data were processed with the nmrPipe package[22] and the spectra were analyzed by using

Sparky software (T. D. Goddard and D. G. Kneller, University of California, San Francisco).

Acknowledgements

We thank K. Senda and K. Hattori (Nagoya City University) for help in the preparation of the recombinant proteins for NMR spectroscopy. We also thank M. Nakano (IMS) and T. Sugihara (JEOL) for help in NMR measurements and K. Matsumoto (RIKEN) for assistance in MS. We thank Drs. H. Sezaki, A. Hayashi, and T. Hosono (Agilent Technologies Japan) for their kind support in liquid chromatography–electrospray ionization MS analysis. This work was supported in part by Grants-in-Aid for Scientific Research on Priority Areas, Research on Pathomechanisms of Brain Disorders (to Y.Y., K.K., and M.H.), Grants-in-Aid for Scientific Research on Innovative Areas, Molecular Science of Fluctuations toward Biological Functions (to K.K.), and "Nanotechnology Network Project" of the Ministry of Education, Culture, Sports, Science and Technology (MEXT). This work was also supported by Takeda Science Foundation (Y.Y.).

Supplementary Data

Supplementary data associated with this article can be found, in the online version, at doi:10.1016/j.jmb.2009.10.068

References

1. Conway, K. A., Rochet, J. C., Bieganski, R. M. & Lansbury, P. T., Jr (2001). Kinetic stabilization of the α-synuclein protofibril by a dopamine-α-synuclein adduct. *Science*, **294**, 1346–1349.
2. Li, H. T., Lin, D. H., Luo, X. Y., Zhang, F., Ji, L. N., Du, H. N. *et al.* (2005). Inhibition of α-synuclein fibrillization by dopamine analogs via reaction with the amino groups of α-synuclein. Implication for dopaminergic neurodegeneration. *FEBS J.* **272**, 3661–3672.
3. Masuda, M., Suzuki, N., Taniguchi, S., Oikawa, T., Nonaka, T., Iwatsubo, T. *et al.* (2006). Small molecule inhibitors of α-synuclein filament assembly. *Biochemistry*, **45**, 6085–6094.
4. Porat, Y., Abramowitz, A. & Gazit, E. (2006). Inhibition of amyloid fibril formation by polyphenols: structural similarity and aromatic interactions as a common inhibition mechanism. *Chem. Biol. Drug Des.* **67**, 27–37.
5. Feng, B. Y., Toyama, B. H., Wille, H., Colby, D. W., Collins, S. R., May, B. C. *et al.* (2008). Small-molecule aggregates inhibit amyloid polymerization. *Nat. Chem. Biol.* **4**, 197–199.
6. Norris, E. H., Giasson, B. I., Hodara, R., Xu, S., Trojanowski, J. Q., Ischiropoulos, H. & Lee, V. M. (2005). Reversible inhibition of α-synuclein fibrillization by dopaminochrome-mediated conformational alterations. *J. Biol. Chem.* **280**, 21212–21219.
7. Herrera, F. E., Chesi, A., Paleologou, K. E., Schmid, A., Munoz, A., Vendruscolo, M. *et al.* (2008). Inhibition of α-synuclein fibrillization by dopamine is mediated by interactions with five C-terminal residues and with E83 in the NAC region. *PLoS ONE*, **e3394**, 3.
8. Ehrnhoefer, D. E., Bieschke, J., Boeddrich, A., Herbst, M., Masino, L., Lurz, R. *et al.* (2008). EGCG redirects amyloidogenic polypeptides into unstructured, off-pathway oligomers. *Nat. Struct. Mol. Biol.* **15**, 558–566.
9. Moussa, C. E., Mahmoodian, F., Tomita, Y. & Sidhu, A. (2008). Dopamine differentially induces aggregation of A53T mutant and wild type α-synuclein: insights into the protein chemistry of Parkinson's disease. *Biochem. Biophys. Res. Commun.* **365**, 833–839.
10. Rao, J. N., Dua, V. & Ulmer, T. S. (2008). Characterization of α-synuclein interactions with selected aggregation-inhibiting small molecules. *Biochemistry*, **47**, 4651–4656.
11. Hong, D. P., Fink, A. L. & Uversky, V. N. (2008). Structural characteristics of α-synuclein oligomers stabilized by the flavonoid baicalein. *J. Mol. Biol.* **383**, 214–223.
12. Masuda, M., Hasegawa, M., Nonaka, T., Oikawa, T., Yonetani, M., Yamaguchi, Y. *et al.* (2009). Inhibition of α-synuclein fibril assembly by small molecules: analysis using epitope-specific antibodies. *FEBS Lett.* **583**, 787–791.
13. Sasakawa, H., Sakata, E., Yamaguchi, Y., Masuda, M., Mori, T., Kurimoto, E. *et al.* (2007). Ultra-high field NMR studies of antibody binding and site-specific phosphorylation of α-synuclein. *Biochem. Biophys. Res. Commun.* **363**, 795–799.
14. Uversky, V. N., Yamin, G., Souillac, P. O., Goers, J., Glaser, C. B. & Fink, A. L. (2002). Methionine oxidation inhibits fibrillation of human α-synuclein *in vitro*. *FEBS Lett.* **517**, 239–244.
15. Paz, M. A., Gallop, P. M., Torrelio, B. M. & Fluckiger, R. (1988). The amplified detection of free and bound methoxatin (PQQ) with nitroblue tetrazolium redox reactions: insights into the PQQ-locus. *Biochem. Biophys. Res. Commun.* **154**, 1330–1337.
16. Ingrosso, D., Fowler, A. V., Bleibaum, J. & Clarke, S. (1989). Specificity of endoproteinase Asp-N (Pseudomonas fragi): cleavage at glutamyl residues in two proteins. *Biochem. Biophys. Res. Commun.* **162**, 1528–1534.
17. Tetaz, T., Morrison, J. R., Andreou, J. & Fidge, N. H. (1990). Relaxed specificity of endoproteinase Asp-N: this enzyme cleaves at peptide bonds N-terminal to glutamate as well as aspartate and cysteic acid residues. *Biochem. Int.* **22**, 561–566.
18. Stadtman, E. R., Van Remmen, H., Richardson, A., Wehr, N. B. & Levine, R. L. (2005). Methionine oxidation and aging. *Biochim. Biophys. Acta*, **1703**, 135–140.
19. Rospigliosi, C. C., McClendon, S., Schmid, A. W., Ramlall, T. F., Barre, P., Lashuel, H. A. & Eliezer, D. (2009). E46K Parkinson's-linked mutation enhances C-terminal-to-N-terminal contacts in α-synuclein. *J. Mol. Biol.* **388**, 1022–1032.
20. Jakes, R., Spillantini, M. G. & Goedert, M. (1994). Identification of two distinct synucleins from human brain. *FEBS Lett.* **345**, 27–32.
21. Masuda, M., Dohmae, N., Nonaka, T., Oikawa, T., Hisanaga, S., Goedert, M. & Hasegawa, M. (2006). Cysteine misincorporation in bacterially expressed human α-synuclein. *FEBS Lett.* **580**, 1775–1779.
22. Delaglio, F., Grzesiek, S., Vuister, G. W., Zhu, G., Pfeifer, J. & Bax, A. (1995). NMRPipe: a multidimensional spectral processing system based on UNIX pipes. *J. Biomol. NMR*, **6**, 277–293.

THE JOURNAL OF BIOLOGICAL CHEMISTRY VOL. 285, NO. 45, pp. 34885–34898, November 5, 2010

Seeded Aggregation and Toxicity of α-Synuclein and Tau

CELLULAR MODELS OF NEURODEGENERATIVE DISEASES[*][S]

Received for publication, May 26, 2010, and in revised form, August 17, 2010 Published, JBC Papers in Press, August 30, 2010, DOI 10.1074/jbc.M110.148460

Takashi Nonaka[‡1], **Sayuri T. Watanabe**[‡§], **Takeshi Iwatsubo**[§¶], **and Masato Hasegawa**[‡2]

From the [‡]*Department of Molecular Neurobiology, Tokyo Institute of Psychiatry, Tokyo 156-8585 and the* [§]*Department of Neuropathology and Neuroscience, Graduate School of Pharmaceutical Science, and* [¶]*Department of Neuropathology, Graduate School of Medicine, University of Tokyo, Tokyo 113-0033, Japan*

The deposition of amyloid-like filaments in the brain is the central event in the pathogenesis of neurodegenerative diseases. Here we report cellular models of intracytoplasmic inclusions of α-synuclein, generated by introducing nucleation seeds into SH-SY5Y cells with a transfection reagent. Upon introduction of preformed seeds into cells overexpressing α-synuclein, abundant, highly filamentous α-synuclein-positive inclusions, which are extensively phosphorylated and ubiquitinated and partially thioflavin-positive, were formed within the cells. SH-SY5Y cells that formed such inclusions underwent cell death, which was blocked by small molecular compounds that inhibit β-sheet formation. Similar seed-dependent aggregation was observed in cells expressing four-repeat Tau by introducing four-repeat Tau fibrils but not three-repeat Tau fibrils or α-synuclein fibrils. No aggregate formation was observed in cells overexpressing three-repeat Tau upon treatment with four-repeat Tau fibrils. Our cellular models thus provide evidence of nucleation-dependent and protein-specific polymerization of intracellular amyloid-like proteins in cultured cells.

The conversion of certain soluble peptides and proteins into insoluble filaments or misfolded amyloid proteins is believed to be the central event in the etiology of a majority of neurodegenerative diseases (1–4). Alzheimer disease (AD)[3] is characterized by the deposition of two kinds of filamentous aggregates, extracellular deposits of β-amyloid plaques composed of amyloid β (Aβ) peptides, and intracellular neurofibrillary lesions consisting of hyperphosphorylated Tau. In Parkinson disease (PD) and dementia with Lewy bodies (DLB), filamentous inclusions consisting of hyperphosphorylated α-synuclein (α-syn) are accumulated in degenerating neurons (5). The deposition of prion proteins in synapses and extracellular spaces is the defining characteristic of Creutzfeldt-Jakob disease and other prion diseases (3). The identification of genetic defects associated with early onset AD, familial PD, frontotemporal dementia, parkinsonism linked to chromosome 17 (caused by Tau mutation and deposition), and familial Creutzfeldt-Jakob disease has led to the hypothesis that the production and aggregation of these proteins are central to the development of neurodegeneration. Fibrils formed of Aβ display a prototypical cross-β-structure characteristic of amyloid (6), as do many other types of filaments deposited in the extracellular space in systemic or organ-specific amyloidoses (7), including prion protein deposits (8). Filaments assembled from α-syn (9) and from Tau filaments (10) were also shown to possess cross-β-structure, as were synthetic filaments derived from exon 1 of huntingtin with 51 glutamines (11). It therefore seems appropriate to consider neurodegenerative disorders developing intracellular deposits of amyloid-like proteins as brain amyloidosis. The accumulation and propagation of extracellular amyloid proteins are believed to occur through nucleation-dependent polymerization (12, 13). However, it has been difficult to establish the relevance of this process in the *in vivo* situation because of the lack of a suitable cell culture model or method to effectively introduce seeds into cells. For example, it has not yet been possible to generate *bona fide* fibrous inclusions reminiscent of Lewy bodies as a model of PD by overexpressing α-syn in neurons of transgenic animals. Here, we describe a novel method for introducing amyloid seeds into cultured cells using lipofection, and we present experimental evidence of seed-dependent polymerization of α-syn, leading to the formation of filamentous protein deposits and cell death. This was also clearly demonstrated in cells expressing different Tau isoforms by introducing the corresponding Tau fibril seeds.

EXPERIMENTAL PROCEDURES

Chemicals and Antibodies—A phosphorylation-independent antibody Syn102 and monoclonal and polyclonal antibodies against a synthetic phosphopeptide of α-syn (Ser(P)^{129}) were used as described previously (5). Polyclonal anti-ubiquitin antibody was obtained from Dako. Polyclonal anti-Tau Ser(P)^{396} was obtained from Calbiochem. Monoclonal anti-α-tubulin and anti-HA clone HA-7 were obtained from Sigma. Lipofectamine was purchased from Invitrogen. Monoclonal

* This work was supported by grants-in-aid for scientific research on Priority Areas, Research on Pathomechanisms of Brain Disorders (to T. I. and M. H.) and Grant-in-aid for Scientific Research (C) 19590297 and 22500345 (to T. N.) from the Ministry of Education, Culture, Sports, Science, and Technology of Japan.

[S] The on-line version of this article (available at http://www.jbc.org) contains supplemental Figs. S1–S5.

[1] To whom correspondence may be addressed: Dept. of Molecular Neurobiology, Tokyo Institute of Psychiatry 2-1-8 Kamikitazawa, Setagaya-ku, Tokyo 156-8585, Japan. Tel.: 81-3-3304-5701; Fax: 81-3-3329-8035; E-mail: nonaka-tk@igakuken.or.jp.

[2] To whom correspondence may be addressed: Dept. of Molecular Neurobiology, Tokyo Institute of Psychiatry 2-1-8 Kamikitazawa, Setagaya-ku, Tokyo 156-8585, Japan. Tel.: 81-3-3304-5701; Fax: 81-3-3329-8035; E-mail: hasegawa-ms@igakuken.or.jp.

[3] The abbreviations used are: AD, Alzheimer disease; Aβ, amyloid β; PD, Parkinson disease; DLB, dementia with Lewy bodies; α-syn, α-synuclein; 3R1N, three-repeat Tau isoform with one amino-terminal insert; 4R1N, four-repeat Tau isoform with one amino-terminal insert; LA, Lipofectamine; LDH, lactate dehydrogenase.

anti-Tau T46 was from Zymed Laboratories Inc.. AT100 and HT7 antibodies were obtained from Innogenetics.

Preparation of α-Syn Seed, Oligomers, and Tau Fibrils—Human α-syn cDNA in bacterial expression plasmid pRK172 was used to produce recombinant protein (14). Wild-type (WT) or carboxyl-terminally HA-tagged α-syn was expressed in *Escherichia coli* BL21 (DE3) and purified as described (15). To obtain α-syn fibrils, α-syn (5–10 mg/ml) was incubated at 37 °C for 4 days with continuous shaking. The samples were diluted with 5 volumes of 30 mM Tris-HCl buffer (pH 7.5) and ultracentrifuged at 110,000 × *g* for 20 min at 25 °C. The pellets were resuspended in 30 mM Tris-HCl buffer (pH 7.5) and sonicated twice for 5 s each. The protein concentration was determined as described, and this preparation was used as Seed αS. In the case of α-syn oligomers, α-syn (10 mg/ml) was incubated at 37 °C for 3 days in the presence of 10 mM exifone. After incubation, the mixture was ultracentrifuged at 110,000 × *g* for 20 min at 25 °C. The supernatant was desalted by Sephadex G-25 (Amersham Biosciences) column chromatography, and eluted fractions (α-syn oligomers) were analyzed by reversed-phase HPLC, SDS-PAGE, and immunoblot analysis. Recombinant human three-repeat Tau isoform with one amino-terminal insert (3R1N) and four-repeat Tau isoform with one amino-terminal insert (4R1N) monomer and corresponding fibrils were prepared as described previously (16, 17).

Introduction of Proteins into Cells—Human neuroblastoma SH-SY5Y cells obtained from ATCC were cultured in DMEM/F-12 medium with 10% FCS. Cells at ~30–50% confluence in 6-well plates were treated with 200 μl of Opti-MEM containing 2 μg of the seed α-syn WT (Seed αS); HA-tagged α-syn (Seed-HA); α-syn monomers, oligomers; or Tau 3R1N or 4R1N fibrils; and 5 μl of Lipofectamine (LA) for 3 h at 37 °C. The medium was changed to DMEM/F-12, and culture was continued for 14 h. The cells were collected by treatment with 0.5 ml of 0.25% trypsin for 10 min at 37 °C, followed by centrifugation (1,800 × *g*, 5 min) and washing with PBS. The cellular proteins were extracted with 100 μl of homogenization buffer containing 50 mM Tris-HCl, pH 7.5, 0.15 M NaCl, 5 mM EDTA, and a mixture of protease inhibitors by sonication. After ultracentrifugation at 290,000 × *g* for 20 min at 4 °C, the supernatant was collected as a Tris-soluble fraction, and the protein concentration was determined by BCA assay. The pellet was solubilized in 100 μl of SDS-sample buffer. Both Tris-soluble and insoluble fractions were analyzed by immunoblotting with appropriate antibodies as indicated (15, 18).

Cell Culture Model of Seed-dependent Polymerization of α-Syn or Tau—α-Syn or Tau 3R1N or 4R1N was transiently overexpressed in SH-SY5Y cells by transfection of 1 μg of wild-type human α-syn cDNA in pcDNA3 (pcDNA3-α-syn) or human Tau cDNA in pcDNA3 (pcDNA3-Tau 3R1N or 4R1N) with 3 μl of FuGENE6 (Roche Applied Science) in 100 μl of Opti-MEM, followed by culture for 14 h. Under our experimental conditions, the efficiency of transfection with pEGFP-C1 vector was 20–30%. The cells were washed with PBS once, and then Seed αS, Seed-HA, Seed 3R1N, or Seed 4R1N was introduced with Lipofectamine as described above. The medium was changed to DMEM/F-12, and culture was continued for ~2–3 days. Cells were harvested in the presence of trypsin to digest extracellular cell-associated α-syn fibrils. The cellular proteins were differentially extracted and immunoblotted with the indicated antibodies, as described (18).

Confocal Microscopy—SH-SY5Y cells on coverslips were transfected with pcDNA3-α-syn and cultured for 14 h as described above, and then Seed αS was introduced, and culture was continued for ~1–2 days. After fixation with 4% paraformaldehyde, the cells were stained with appropriate primary and secondary antibodies as described previously (18). For thioflavin S staining, the cells were incubated with 0.05% thioflavin S at room temperature for 5 min. Fluorescence was analyzed with a laser-scanning confocal fluorescence microscope (LSM5Pascal, Carl Zeiss).

Immunoelectron Microscopy—For electron microscopy, cells overexpressing α-syn were transfected with Seed αS, cultured for 2 days, fixed in 0.1 M phosphate buffer containing 4% glutaraldehyde for 12 h, and then processed and embedded in LR White resin (London Resin, Reading, UK). Ultrathin sections were stained with uranyl acetate for investigation. Immunolabeling of the inclusions was performed by means of an immunogold-based postembedding procedure. Sections were blocked with 10% calf serum, incubated overnight on grids with anti-Ser(P)^{129} antibody at a dilution of 1:100, rinsed, then reacted with secondary antibody conjugated to 10-nm gold particles (E-Y Laboratories, San Mateo, CA) (1:10), rinsed again and stained with uranyl acetate.

Immunoelectron microscopic analysis of α-syn or Tau filaments extracted from cells was performed as follows. Cells overexpressing α-syn or Tau were transfected with Seed αS or Seed Tau, respectively. After incubation for 3 days, they were harvested, suspended in 200 μl of 10 mM Tris-HCl, pH 7.4, 1 mM EGTA, 10% sucrose, 0.8 M NaCl) and sonicated. The lysates were centrifuged at 20,400 × *g* for 20 min at 4 °C. The supernatant was recovered, and Sarkosyl was added (final 1%, v/v). The mixtures were incubated at room temperature for 30 min and then centrifuged at 113,000 × *g* for 20 min. The resulting pellets were suspended in 30 mM Tris-HCl, pH 7.5, placed on collodion-coated 300-mesh copper grids, and stained with the indicated antibodies and 2% (v/v) phosphotungstate. Micrographs were recorded on a JEOL 1200EX electron microscope.

Cell Death Assay—Cell death assay was performed using a CytoTox 96 non-radioactive cytotoxicity assay kit (Promega). TUNEL staining was performed using an *in situ* cell death detection kit (Roche Applied Science).

Assay of Proteasome Activity—SH-SY5Y cells transfected with pcDNA3-α-syn and Seed αS were cultured for 3 days or treated with 20 μM MG132 for 4 h. Cells were harvested, and cytosolic fraction was prepared as follows. Cells were resuspended in 100 μl of phosphate-buffered saline (PBS) and disrupted by sonication, and then insoluble material was removed by ultracentrifugation at 290,000 × *g* for 20 min at 4 °C. The supernatant was assayed for proteasome activity by using a fluorescent peptide substrate, benzyloxycarbonyl-Leu-Leu-Glu-7-amido-4-methylcoumarin (Peptide Institute, Inc.). 7-Amino-4-methylcoumarin release was measured fluorometrically (excitation at 365 nm; emission at 460 nm). In a green fluorescent protein (GFP) reporter assay of proteasome activity in living cells by confocal laser microscopy, SH-SY5Y cells trans-

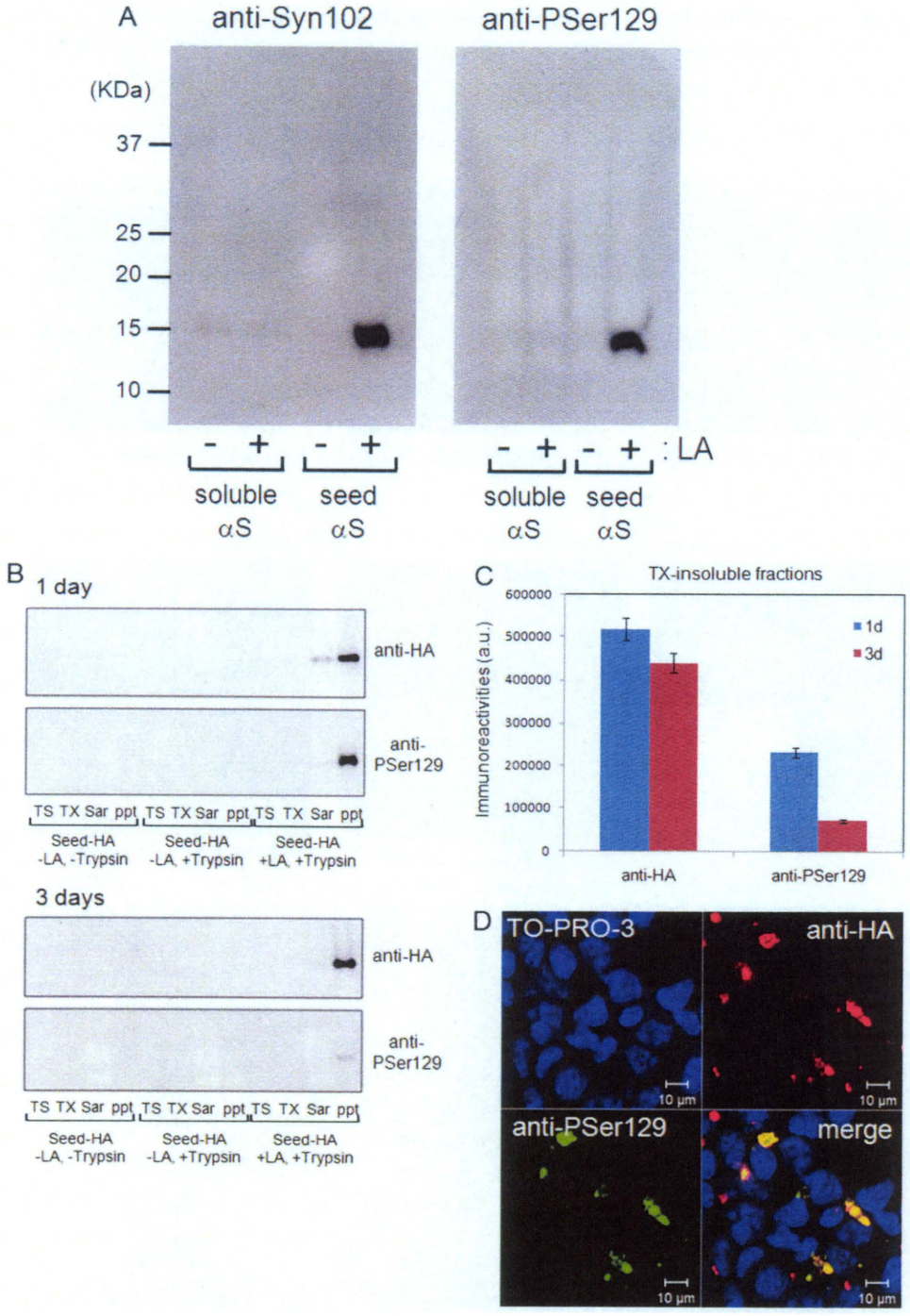

FIGURE 1. **Introduction of seed α-syn into cultured cells with Lipofectamine reagent.** *A*, purified recombinant α-syn (soluble form; 2 μg) and filaments (2 μg) were sonicated and then incubated with LA. The protein-LA complexes were dispersed in Opti-MEM and added to SH-SY5Y cells. After 14 h of culture, the cells were collected and sonicated in SDS sample buffer. After boiling, the samples were analyzed by immunoblotting with a phosphorylation-dependent anti-α-syn Ser(P)^{129} (*PSer129*) (*right*) or a phosphorylation-independent antibody, Syn102 (*left*). *B* and *C*, carboxyl-terminally HA-tagged α-syn fibril seeds (*Seed-HA*) were transduced into cells by the use of LA. After incubation for 1 day (*1d*) or 3 days (*3d*), cells were harvested with or without trypsin, and proteins were differentially extracted from the cells with Tris-HCl (*TS*), Triton X-100 (*TX*), and Sarkosyl (*Sar*), leaving the pellet (*ppt*). Immunoblot analyses of lysates using anti-HA and anti-Ser(P)^{129} are shown. The immunoreactive band positive for anti-HA or anti-Ser(P)^{129} in the Triton X-100-insoluble fraction was quantified. The results are expressed as means ± S.E. ($n = 3$). *D*, confocal laser microscopic analysis of cells treated with Seed-HA in the presence of LA. Cells were transduced with 2 μg of Seed-HA using 5 μl of LA. After a 48-h incubation, cells were fixed and immunostained with anti-Ser(P)^{129} (*green*) and anti-HA (*red*) and counterstained with TO-PRO-3 (*blue*).

fected with pcDNA3-α-syn (1 μg) and GFP-CL1 (0.3 μg) using FuGENE6 and then transfected with Seed αS were grown on coverslips for 2 days or treated with 20 μM MG132 for 6 h (19). These cells were analyzed using a laser-scanning confocal fluorescence microscope (LSM5Pascal, Carl Zeiss).

Statistical Analysis—The p values for the description of the statistical significance of differences were calculated by means of the unpaired, two-tailed Student's t test using GraphPad Prism 4 software (GraphPad Software).

RESULTS

Introduction of Seed α-Syn into Cultured Cells Using Lipofectamine Reagent—Cellular overexpression of α-syn by itself does not lead to fibrillization of α-syn in a form that resembles Lewy bodies. This prompted us to examine whether or not introduction of preformed aggregation seeds of α-syn (Seed αS) would elicit fibril formation. To introduce Seed αS into SH-SY5Y cells in a non-invasive manner, we tried several reagents used for transporting proteins or plasmid DNA into cells and found that LA, a cationic gene introducer, enables the introduction of Seed αS into SH-SY5Y cells. We were not able to detect any introduced α-syn monomer or fibrils following the simple addition of protein preparations to the culture medium, notwithstanding a previous report on this approach (20). The insoluble α-syn formed following LA-mediated Seed αS introduction was detected as buffer-insoluble α-syn in cell lysates (Fig. 1*A*). The insoluble α-syn was phosphorylated at Ser^{129} upon introduction into cells (Fig. 1*A*), indicating that Seed αS was incorporated in cells and phosphorylated intracellularly. Cells were harvested in the presence of trypsin to digest extracellular cell-associated α-syn fibrils. The optimal ratio of LA to Seed αS was about 5 μl to 2 μg of protein in 6-well plates. This treatment effectively introduced Seed αS not only into SH-SY5Y cells but also into several other types of cells examined, including Chinese hamster ovary cells and human embryonic kidney 293T cells (data not shown). In sharp contrast, soluble α-syn (either monomeric or oligomeric forms) was not introduced into the

cells by the same treatment (Figs. 1*A* and 4), suggesting that the LA treatment works exclusively for the internalization of insoluble α-syn aggregates.

These results strongly suggest that α-syn fibrils are incorporated with the aid of LA but do not exclude the possibility that extracellular α-syn fibrils may induce aggregation of endogenous α-syn without incorporation. To confirm that the extracellular α-syn fibril seeds are internalized into cells by LA, we performed the transduction of preformed carboxyl-terminally HA-tagged α-syn fibril seeds (Seed-HA) instead of non-tagged

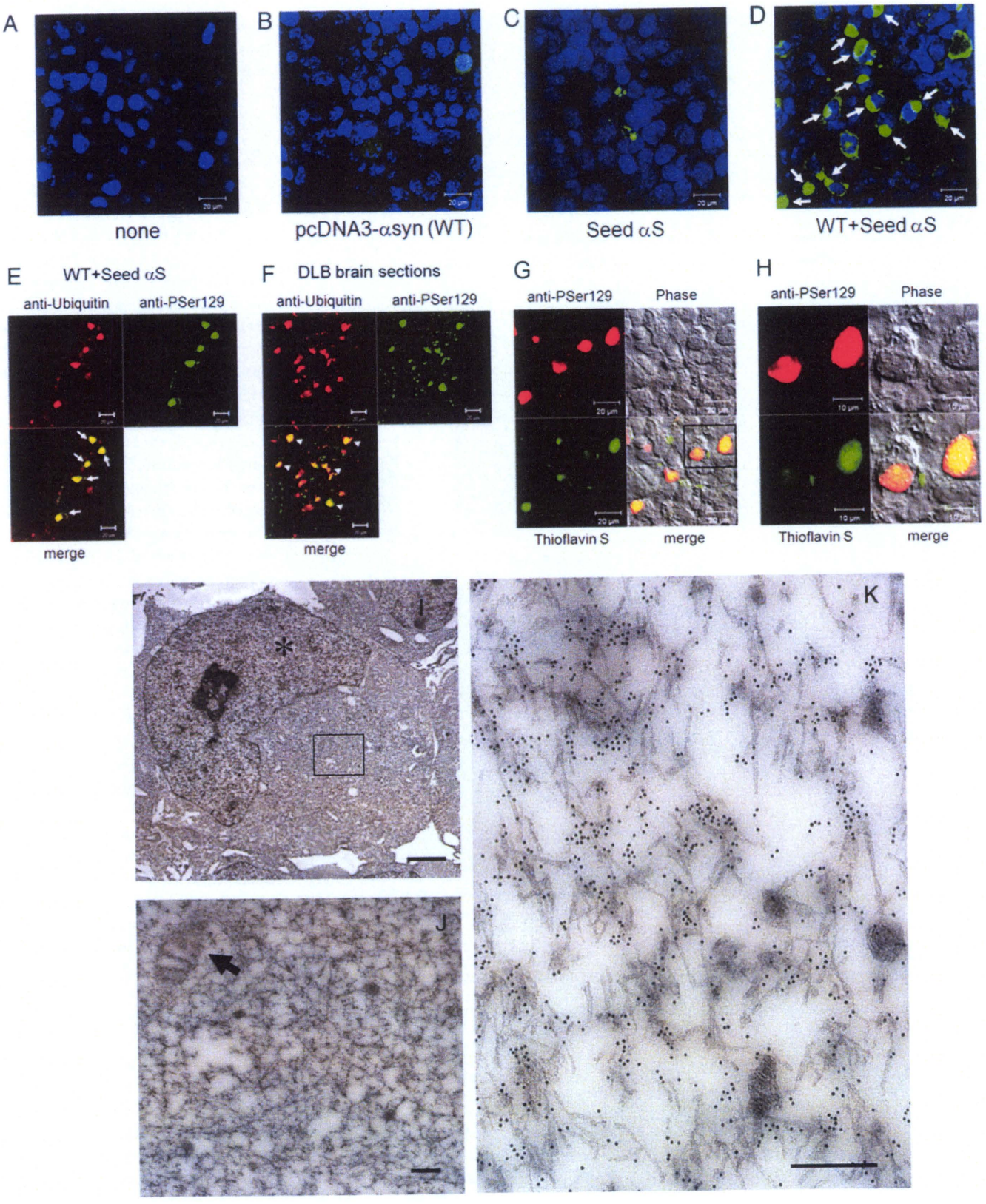

α-syn seeds. As shown in Fig. 1, *B* and *C*, time course experiments revealed that Seed-HA was also incorporated into cells in the presence of LA and could be detected with both anti-HA antibody and a phospho-α-syn-specific antibody (anti-Ser(P)^{129}), even 3 days after infection. Confocal microscopic analyses also indicated that Seed-HA was phosphorylated at Ser^{129} intracellularly. All anti-Ser(P)^{129}-positive dotlike structures were also stained with anti-HA, indicating that no endogenously phosphorylated α-syn aggregates are present in the cells (Fig. 1*D* and supplemental Fig. S1*C*).

Establishment of a Cell Culture Model for Nucleation-dependent Polymerization of α-Syn—Although introduction of the seed α-syn into cells was accompanied with phosphorylation, no further dramatic change was observed. Because the level of endogenous α-syn was relatively low in SH-SY5Y cells, we introduced non-tagged or HA-tagged seeds into cells transiently overexpressing α-syn. After 3 days of culture, immunocytochemistry for α-syn revealed a diffuse (Fig. 2*B*) or dotlike (Fig. 2*C*) pattern of cytoplasmic labeling by anti-Ser(P)^{129} in cells transfected with wild-type α-syn without seeds or in non-overexpressing cells with Seed αS, respectively. Surprisingly, however, in cells transfected with both pcDNA3-α-syn and Seed αS, we observed abundant round inclusions that occupied the cytoplasm and displaced the nucleus, with morphology highly reminiscent of cortical-type Lewy bodies observed in human brain (Fig. 2*D*). The size of the α-syn-positive inclusions was ~10 μm in diameter (Fig. 2*D*), which is similar to that of the Lewy bodies detected in the brains of patients with dementia with Lewy bodies. Similarly, when cells expressing α-syn were transfected with Seed-HA, abundant phosphorylated α-syn-positive cells were also detected (supplemental Fig. S1*D*).

We next examined the status of ubiquitin, which is positive in most types of intracellular filamentous inclusions, including Lewy bodies, in neurodegenerative disease brains. As shown in Fig. 2*E*, we found that almost all intracellular inclusions labeled with anti-Ser(P)^{129} were also positive for ubiquitin, as is the case for Lewy bodies in the cortex of human DLB brain (Fig. 2*F*). Furthermore, the juxtanuclear Ser(P)^{129}-positive, Lewy body-like inclusions were also positively labeled with thioflavin S, a fluorescent dye that specifically intercalates within structures rich in β-pleated sheet conformation (Fig. 2, *G* and *H*), indicating that the inclusions contain β-sheet-rich filamentous aggregates. Electron microscopic analysis of cells transfected with both wild-type α-syn and the seeds revealed that the inclusions are composed of filamentous structures ~10 nm in diameter that are often covered with granular materials (Fig. 2, *I* and *J*). The filamentous structures were randomly oriented within the cytoplasm of these cells, forming a meshwork-like profile, and were frequently intermingled with mitochondria (Fig. 2, *I* and *J*), being highly reminiscent of human cortical Lewy bodies. Immunoelectron microscopy showed that the filaments were densely decorated with anti-Ser(P)^{129} (Fig. 2*K*), demonstrating that they were composed of phosphorylated α-syn.

To biochemically validate this cellular model and to investigate further the molecular mechanisms underlying nucleation-dependent aggregation within cells, we differentially extracted α-syn from these cells using detergents of various strengths and analyzed the extracts by immunoblotting with anti-Syn102 and -Ser(P)^{129} antibodies. The levels of α-syn in the Sarkosyl-soluble and -insoluble fractions (total α-syn and α-syn phosphorylated at Ser^{129}, respectively) were dramatically increased in cells transfected with both wild-type α-syn and the seeds (*WT + Seed αS* in Fig. 3, *A* and *B*). To distinguish endogenous α-syn from exogenous α-syn fibrils, we used LA to transduce Seed-HA into cells overexpressing α-syn. Immunoblot analyses of these cells showed that HA-tagged α-syn with slower mobility than non-tagged α-syn was detected in the Sarkosyl-insoluble pellets as phosphorylated forms by anti-HA and anti-Ser(P)^{129} antibodies in cells treated with Seed-HA + LA (Fig. 3, *C–E*). Interestingly, in cells expressing α-syn (WT) treated with Seed-HA + LA, much more abundant non-tagged α-syn was detected in the Triton X-100- and Sarkosyl-insoluble fractions as phosphorylated forms with a smaller amount of the HA-α-syn. We also performed a dose dependence experiment with Seed-HA in cells expressing α-syn. As shown in supplemental Fig. S2, immunoreactive levels of Triton X-100-insoluble phosphorylated α-syn increased in parallel with an increase in the amount of Seed-HA. Furthermore, we tested whether Tau protein forms intracellular aggregates in the presence of α-syn seeds instead of Tau seeds. We found that Tau was not aggregated with Seed-HA, confirming that intracellular aggregate formation of soluble α-syn is specific to and dependent on fibril seeds of the same protein (supplemental Fig. S3). This nucleation-dependent polymerization of α-syn in cells was greater at 3 days than at 1 day after transduction of the seeds (Fig. 3*F*).

Negative stain electron microscopic observation of Sarkosyl-insoluble fractions of the cells harboring inclusions revealed anti-Syn102 and Ser(P)^{129}-positive filaments of ~5–10-nm width (Fig. 3, *G* and *H*) that are highly reminiscent of those derived from human α-synucleinopathy brains (21). Such filaments were never detected in the Sarkosyl-insoluble fraction of cells solely overexpressing α-syn (data not shown). These results indicated that the biochemical characteristics of α-syn accumulated in cells forming the Lewy body-like inclusions

FIGURE 2. **Confocal laser and electron microscopic analyses of α-syn inclusions in plasmid-derived α-syn-expressing cells treated with seed α-syn.** *A–D*, confocal laser microscopic analyses of control SH-SY5Y cells transfected with pcDNA3 vector and Lipofectamine alone (*A*), cells transfected with pcDNA3-α-syn (*WT*) (*B*), cells transduced with the seed α-syn (*Seed αS*) (*C*), and cells transfected with both pcDNA3-α-syn and Seed αS (*WT + Seed αS*) (*D*), immunostained with anti-Ser(P)^{129} (*green*), and counterstained with TO-PRO-3 (*blue*). The *arrows* indicate cytoplasmic round inclusions stained with anti-Ser(P)^{129} (*PSer129*). *Scale bars*, 20 μm. *E–F*, comparison of confocal images of cells transfected with both α-syn plasmid and Seed αS (*E*) and tissue sections from DLB brains (*F*) using anti-Ser(P)^{129} (*green*) and anti-ubiquitin antibodies (*red*). Cytoplasmic inclusions in transfected cells (*arrows*) are positive for ubiquitin, like Lewy bodies (*arrowheads*) in DLB brains. *Scale bars*, 20 μm. *G* and *H*, confocal microscopic images of cells transfected with both pcDNA3-α-syn and Seed αS. Cells were stained with 0.05% Thioflavin S (*green*) and anti-Ser(P)^{129} antibody (*red*). The *boxed area* on the *left* is shown in the *right panel*. *Scale bars*, 20 μm on the *left* and 10 μm on the *right*. *I* and *J*, electron microscopic analyses of cells transfected with both pcDNA3-α-syn and Seed αS. High magnification of the boxed area in *I* is shown in *J*. An *asterisk* or *arrow* indicates a nucleus or mitochondrion, respectively. *Scale bars*, 2 μm in *I* and 200 nm in *J*. *K*, immunoelectron microscopic observation of cells transfected with both pcDNA3-α-syn and Seed αS using a polyclonal antibody against phosphorylated Ser^{129} of α-syn. *Scale bar*, 200 nm.